Inorg. Chem. **2005**, *44*, 6159–6173

Tunable DNA Photocleavage by an Acridine–Imidazole Conjugate

Beth Wilson,[†] Lourdes Gude,[‡] María-José Fernández,[‡] Antonio Lorente,*[,‡] and Kathryn B. Grant*[,†]

Department of Chemistry, Center for Biotechnology and Drug Design, Georgia State University, P.O. Box 4098, Atlanta, Georgia 30302-4098, and Departamento de Química Orgánica, Universidad de Alcalá, 28871-Alcalá de Henares, Madrid, Spain

Received November 28, 2004

We report the synthesis and characterization of photonucleases *N*,*N*′-bis[2-[bis(1*H*-imidazol-4-ylmethyl)amino]ethyl]-3,6-acridinediamine (**7**) and *N*-[2-[bis(1*H*-imidazol-4-ylmethyl)amino]ethyl]-3,6-acridinediamine (**10**), consisting of a central 3,6-acridinediamine chromophore attached to 4 and 2 metal-coordinating imidazole rings, respectively. In DNA reactions employing 16 metal salts, photocleavage of pUC19 plasmid is markedly enhanced when compound **7** is irradiated in the presence of either Hg(II), Fe(III), Cd(II), Zn(II), V(V), or Pb(II) (low-intensity visible light, pH 7.0, 22 °C, 8–50 μM **7**). We also show that DNA photocleavage by **7** can be modulated by modifying buffer type and pH. Evidence of metal complex formation is provided by EDTA experiments and by NMR and electrospray ionization mass spectral data. Sodium azide, sodium benzoate, superoxide dismutase, and catalase indicate the involvement of type I and II photochemical processes in the metal-assisted DNA photocleavage reactions. Thermal melting studies show that compound **7** increases the T_m of calf thymus DNA by 10 ± 1 °C at pH 7.0 and that the T_m is further increased upon the addition of either Hg(II), Cd(II), Zn(II), or Pb(II). In the case of Fe(III) and V(V), a colorimetric assay demonstrates that compound **7** sensitizes one electron photoreduction of these metals to Fe(II) and V(IV), likely accelerating the production of type I reactive oxygen species. Our data collectively indicate that buffer, pH, Hg(II), Fe(III), Cd(II), Zn(II), V(V), Pb(II), and light can be used to "tune" DNA cleavage by compound **7** under physiologically relevant conditions. The 3,6-acridinediamine acridine orange has demonstrated great promise for use as a photosensitizer in photodynamic therapy. In view of the distribution of iron in living cells, compound **7** and other metal-binding acridine-based photonucleases should be expected to demonstrate excellent photodynamic action in vivo.

Introduction

Photodynamic therapy (PDT) has been proven to be an effective treatment option for age-related macular degeneration, actinic keratoses, as well as for neoplastic diseases such as lung, bladder, and esophageal cancers.[1] PDT is also being explored for its potential application in the photoinactivation of viruses (e.g., in blood disinfection) and of multidrug resistant bacteria.[2] The procedure involves the administration of a photoactive drug (photosensitizer) either systemically or topically followed by irradiation of target tissue with light wavelengths specifically absorbed by the photosensitizer. Damage to surrounding healthy tissue is mitigated by the preferential accumulation and activation of the photosensitizer in diseased tissue. In this regard, PDT represents a very attractive alternative to conventional chemotherapy. Nevertheless, only a few drugs, mostly first and second generation porphyrin derivatives, have been approved for clinical use in PDT.[1a,3] The most extensively researched and utilized is

* To whom correspondence should be addressed. E-mail: antonio.lorente@uah.es (A.L.); kbgrant@gsu.edu (K.B.G.). Fax: 34 91 885 46 86 (A.L.); 1-404-651-1416 (K.B.G.).

[†] Georgia State University.

[‡] Universidad de Alcalá.

(1) (a) Dolmans, D. E. J. G. J.; Fukumura, D.; Jain, R. K. *Nat. Rev. Cancer* **2003**, *3*, 380−387. (b) Stapleton, M.; Rhodes, L. E. *J. Dermatolog. Treat.* **2003**, *2*, 107−112. (c) Vrouenraets, M. B.; Visser, G. W. M.; Snow, G. B.; van Dongen, G. A. M. S. *Anticancer Res.* **2003**, *23*, 505−522. (d) Zeitouni, N. C.; Oseroff, A. R.; Shieh, S. *Mol. Immunol.* **2003**, *39*, 1133−1136. (e) Dougherty, T. J. *J. Clin. Laser. Med. Surg.* **2002**, *20*, 3−7. (f) Fong, D. S. *Ophthalmology* **2000**, *107*, 2314−2317.

(2) (a) Ashkenazi, H.; Nitzan, Y.; Gál, D. *Photochem. Photobiol.* **2003**, *77*, 186−191. (b) Wainwright, M. *Int. J. Antimicro. Agents* **2003**, *21*, 510−520. (c) Ramaiah, D.; Eckert, I.; Arun, K. T.; Weidenfeller, L.; Epe, B. *Photochem. Photobiol.* **2002**, *76*, 672−677. (d) Wagner, S. J.; Skripchenko, A.; Thompson-Montgomery, D. *Photochem. Photobiol.* **2002**, *76*, 514−517. (e) Smetana, Z.; Ben-Hur, E.; Mendelson, E.; Salzberg, S.; Wagner, P.; Malik, Z. *J. Photochem. Photobiol., B: Biol.* **1998**, *44*, 77−83.

10.1021/ic048320x CCC: $30.25
Published on Web 08/11/2005

Photofrin. Yet, large doses of this porphyrin are required to achieve therapeutic efficacy, the identity of the active component(s) has not been determined, and the drug causes prolonged periods of skin photosensitivity.[4] There is now a great interest in the development of new photoactive drugs that are therapeutically more effective and less toxic.

Following the absorption of a photon of light, PDT sensitizer molecules are excited to a high energy singlet state. Subsequent intersystem crossing yields a long-lived excited triplet state which can undergo energy transfer with ground-state molecular oxygen to generate cytotoxic singlet oxygen ($^1O_2$; type II reaction). Alternatively, the photosensitizer triplet participates in one electron oxidation of a nearby substrate such as DNA (type I reaction). In the case of molecular oxygen, type I electron transfer from the triplet to O_2 produces superoxide ($O_2^{\bullet -}$), which reacts further to generate hydrogen peroxide and cytotoxic hydroxyl radicals ($OH^{\bullet}$). Although type I processes play a relatively minor role in PDT compared to type II, singlet oxygen, hydroxyl radicals, and one electron oxidation can all cause significant damage to DNA and other biomolecules, eventually effecting necrosis and/or apoptosis of targeted cells.[5] In addition, recent investigations indicate that PDT may function by triggering localized inflammatory cell and immune reaction responses.[6]

A precondition for efficacious photodynamic activity is selective and preferential retention of the photosensitizer in diseased tissue. This prerequisite is met by sensitizing chromophores that bind to nucleic acids with high affinity. The acridines are well-known DNA intercalating drugs that possess photo- and cytotoxic properties. The 3,6-acridinediamines acridine orange and proflavin have been shown to photocleave DNA[7] as a function of increasing nucleic acid bound chromophore.[7a,c] Furthermore, acridine orange has demonstrated selective localization in a number of tumor types and has effected efficient in vivo photodestruction of epithelial tumors in mice, Walker carcinosarcoma 256 stomach tumors in rats, and musculoskeletal sarcomas in mice.[8] In fact, Tatsuta et al. reported comparable PDT-mediated necrosis of rat carcinosarcoma stomach tumors by both acridine orange and hematoporphyrin.[8c] Finally, second and third generation acridines have produced cytotoxic effects

Scheme 1 [a]

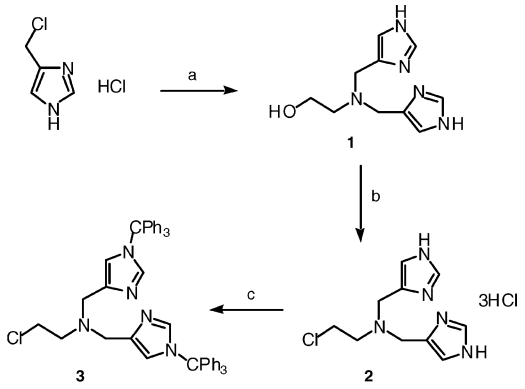

[a] Conditions: (a) $HOCH_2CH_2NH_2$, EtOH, Et_3N, reflux, 70%; (b) $SOCl_2$, DMF, rt, 86%; (c) Ph_3CCl, Et_3N, DMF, rt, 61%.

in a variety of cancerous tissues and are being developed as HIV antivirals.[9]

In view of the close association of iron and other metals with genomic DNA[10] and the coaccumulation of iron and acridine orange in lysosomes and the cell nucleus,[11] acridine-based photonucleases that sequester metals are potentially of great utility in living cells. Toward this end, we report the syntheses of compounds **7** and **10**, containing a central DNA-binding 3,6-acridinediamine chromophore attached to 4 and 2 metal-coordinating imidazole rings, respectively. In a survey of 16 metal salts, we demonstrate that the in vitro DNA-photocleaving properties of compound **7** are markedly enhanced by specific ions in the approximate order Fe(III) $\approx$ Hg(II) > Cd(II) > Zn(II) > V(V) $\approx$ Pb(II). In the presence of these metals, pUC19 plasmid DNA is readily converted into its nicked form upon exposure to low-intensity, visible light (pH 7.0, 22 °C, 8−50 μM **7**).

Results and Discussion

Synthesis.[12] The tetraimidazole derivative of 3,6-acridinediamine **7** was synthesized according to the procedures depicted in Schemes 1 and 2. In the first step of the synthetic route, 2-[bis(1*H*-imidazol-4-ylmethyl)amino]ethanol (**1**) was obtained by reaction of 4-(chloromethyl)-1*H*-imidazole hydrochloride with 2-aminoethanol in refluxing ethanol. Afterward, a solution of **1** in dry DMF with thionyl chloride

(3) Bonnet, R. In *Chemical Aspects of Photodynamic Therapy*; Phillips, D., Ed.; Gordon and Breach Science: Amsterdam, 2000; Vol. I, pp 70−87.
(4) (a) Konan, Y. N.; Gurny, R.; Allémann, E. *J. Photochem. Photobiol., B: Biol.* **2002**, *66*, 89−106. (b) Zovinka, E. P.; Sunseri, D. R. *J. Chem. Educ.* **2002**, *79*, 1331−1335. (c) Schuitmaker, J. J.; Baas, P.; van Leegoed, H. L. L. M.; van der Meulen, F. W.; Star, W. M.; van Zandwijk, N. *J. Photochem. Photobiol., B: Biol.* **1996**, *34*, 3−12.
(5) (a) Quédraogo, G. D.; Redmond, R. W. *Photochem. Photobiol.* **2003**, *77*, 192−203. (b) Choi Kim, H. R.; Luo, Y.; Li, G.; Kessel, D. *Cancer Res.* **1999**, *59*, 3429−3432. (c) Ochsner, M. *J. Photochem. Photobiol., B: Biol.* **1997**, *39*, 1−18.
(6) (a) Gollnick, S. O.; Evans, S. S.; Baumann, H.; Owczarczak, B.; Maier, P.; Vaughan, L.; Wang, W. C.; Unger, E.; Henderson, B. W. *Br. J. Cancer* **2003**, *88*, 1772−1779. (b) Korbelik, M.; Dougherty, G. J. *Cancer Res.* **1996**, *59*, 1941−1946.
(7) (a) Bowler, B. E.; Hollis, S.; Lippard, S. J. *J. Am. Chem. Soc.* **1984**, *106*, 6102−6104. (b) Piette, J.; Lopez, M.; Calberg-Bacq, C. M.; Van de Vorst, A. *Int. J. Radiat. Biol.* **1981**, *40*, 427−433. (c) Piette, J.; Calberg-Bacq, C. M.; Van de Vorst, A. *Photochem. Photobiol.* **1979**, *30*, 369−378. (d) Freifelder, D.; Davison, P. F.; Geiduschek, E. P. *Biophys. J.* **1961**, *1*, 389−400.
(8) (a) Kusuzaki, K.; Aomori, K.; Suginoshita, T.; Minami, G.; Takeshita, H.; Murata, H.; Hashiguchi, S.; Ashihara, T.; Hirasawa, Y. *Oncology* **2000**, *59*, 174−180. (b) Kusuzaki, K.; Suginoshita, T.; Minami, G.; Aomori, K.; Takeshita, H.; Murata, H.; Hashiguchi, S.; Ashihara, T.; Hirasawa, Y. *Anticancer Res.* **2000**, *20*, 3019−3024. (c) Tatsuta, M.; Iishi, H.; Yamamura, H.; Yamamoto, R.; Okuda, S. *Oncology* **1988**, *45*, 35−40. (d) Tatsuta, M.; Yamamura, H.; Yamamoto, R.; Ichii, M.; Noguchi, S.; Iishi, H.; Mishima, H.; Hattori, T.; Okuda, S. *Eur. J. Cancer Clin. Oncol.* **1984**, *20*, 543−552. (e) Tomson, S. H.; Emmett, E. A.; Fox, S. H. *Cancer Res.* **1974**, *34*, 3124−3127.
(9) (a) Malinina, L.; Soler-López, M.; Aymamí, J.; Subirana, J. A. *Biochemistry* **2002**, *41*, 9341−9348. (b) Mazerska, Z.; Dziegielewski, J.; Konopa, J. *Biochem. Pharmacol.* **2001**, *61*, 685−694. (c) Giménez-Arnau, E.; Missailidis, S.; Stevens, M. F. G. *Anti-Cancer Drug Des.* **1998**, *13*, 431−451.
(10) Bregadze, V.; Khutsishvili, I.; Chkhaberidze, J.; Sologhashvili, K. *Inorg. Chim. Acta* **2002**, *339*, 145−159.
(11) Kurz, T.; Leake, A.; von Zglinicki, T.; Brunk, U. T. *Ann. N.Y. Acad. Sci.* **2004**, *1019*, 285−288.
(12) Lorente, A.; Espinosa, J. F.; Fernández-Saiz, M.; Lehn, J.-M.; Wilson, W. D.; Zhong, Y. Y. *Tetrahedron Lett.* **1996**, *37*, 4417−4420.

Scheme 2 [a]

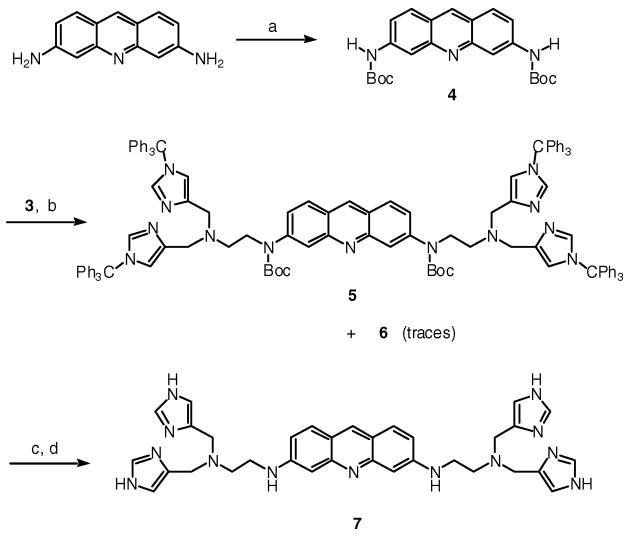

[a] Conditions: (a) ^{t}BuOOCOCOO^{t}Bu, acetone, reflux, 72%; (b) Cs_2CO_3, DMF, rt, 89%; (c) 2 N HCl, 60 °C; (d) 2 N NaOH, 87%.

Scheme 3 [a]

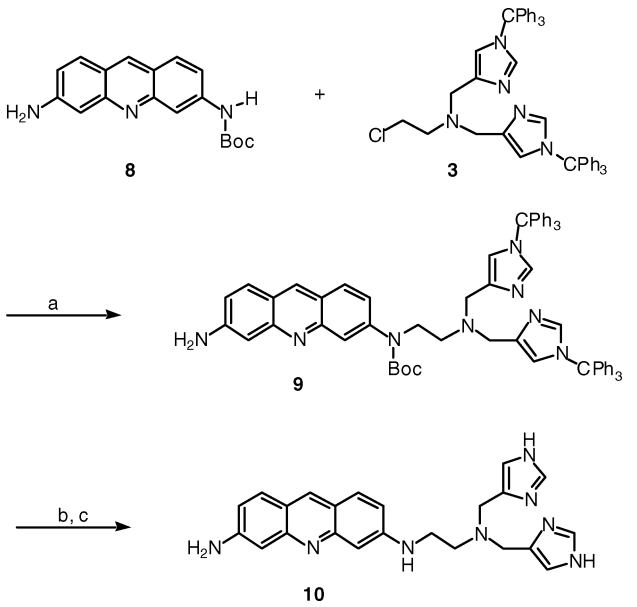

[a] Conditions: (a) Cs_2CO_3, DMF, rt, 85%; (b) 2 N HCl, 60 °C; (c) 2 N NaOH, 70%.

was stirred at room temperature for 24 h to yield *N*-(2-chloroethyl)-*N*-(1*H*-imidazol-4-ylmethyl)-1*H*-imidazole-4-methanamine trihydrochloride (**2**).

Next, several attempts were made to accomplish the straightforward synthesis of **7** by reaction of 3,6-acridinediyl-bis(carbamic acid) bis(1,1-dimethylethyl) ester (**4**) with **2** in the presence of different bases but with no success. The basic conditions required for proflavin dicarbamate alkylation made previous protection of the imidazole nitrogen advisable. Therefore, we proceeded to protect it regioselectively by using the triphenylmethyl group (Scheme 1), a robust protecting group under basic conditions that can be easily removed by acid hydrolysis.

We then evaluated conditions for the reaction of protected derivative **3** with dicarbamate **4**. Although we initially employed sodium hydride in DMF, which afforded a mixture of the di- (**5**) and monoalkylated (**6**) products (in 54 and 32% yields, respectively), a more convenient approach resulted from substitution of NaH with Cs_2CO_3 (Scheme 2). This simplified the workup process and increased the reaction yield. Finally, all the protecting groups were removed simultaneously by treatment of **5** at 60 °C with 2 N hydrochloric acid. After basification of the reaction mixture, *N*,*N*′-bis[2-[bis(1*H*-imidazol-4-ylmethyl)amino]ethyl]-3,6-acridinediamine (**7**) was precipitated and purified.

The synthesis of bisimidazolic proflavin derivative **10** was carried out following a similar procedure (Scheme 3). Compound **9** was prepared through the reaction of (6-amino-3-acridinyl)carbamic acid 1,1-dimethylethyl ester (**8**) with **3** using cesium carbonate as base and dry DMF as solvent. Deprotection with 2 N hydrochloric acid at 60 °C afforded, after basification with aqueous sodium hydroxide, *N*-[2-[bis-(1*H*-imidazol-4-ylmethyl)amino]ethyl]-3,6-acridinediamine (**10**).

^{1}H NMR Spectroscopy. To obtain evidence of complex formation, NMR spectra were recorded for 5.7 mM of compound **7** as function of increasing $ZnCl_2$ concentration (300 MHz, CD_3OD). At 5.7 mM Zn(II) (1:1 metal-to-ligand ratio), integration of the H-2 and H-5 imidazole signals revealed than only two of the four protons were downfield shifted, suggesting the formation of a stoichiometric 1:1 species. (Chemical shifts were 7.58 and 6.94 ppm with no metal ion and 8.00 and 7.22 ppm with metal, respectively.) At a 2:1 metal-to-ligand ratio, the downfield shifts were observed for all the H-2 and H-5 proton signals, indicating a 2:1 metal to ligand complex. No additional changes in the NMR spectra were seen at zinc(II) concentrations higher than 11.4 mM.

Mass Spectrometry. Electrospray ionization (ESI) mass spectrometry is routinely used for the detection of labile metal complexes in situ. To allow for varied stoichiometries, we prepared electrospray samples by mixing different volumes of 0.4 mM methanolic stock solutions of **7** and a metal salt (either $CdCl_2$, $FeCl_3 \cdot 6H_2O$, $HgCl_2$, Na_3VO_4, $PbCl_2$, or $ZnCl_2$) in pure HPLC grade methanol. The samples were then allowed to equilibrate at room temperature for 45 min, after which mass spectra were recorded. In the case of $ZnCl_2$ and $CdCl_2$, the major isotopic peaks were found to correspond to the following: 1:1 metal-to-ligand complex and unreacted **7** at a metal-to-ligand ratios of 1:2; 1:1 metal-to-ligand complex, 2:1 complex, and unreacted **7** at metal-to-ligand ratios of 1:1; 2:1 metallic complex at metal-to-ligand ratios of 2:1. Alternatively, the major isotopic peaks of $HgCl_2$ and $PbCl_2$ indicated the formation of a 1:1 metal-to-ligand complex and unreacted **7** at metal-to-ligand ratios of 1:2, and a gradual conversion of unreacted **7** to 1:1 complex as the ratios of metal-to-ligand were increased to 1:1 and then to 2:1. In the case of $FeCl_3 \cdot 6H_2O$, there was no evidence of complex formation at metal-to-ligand ratios of 1:2 and 1:1. However, at the 1:2 ratio, minor isotopic peaks corresponding to a 1:1 complex were observed. Although attempts to study vanadium(V) complex formation were unsuccessful in neat methanol, low levels of a 1:1 metal-to-ligand complex were seen at all metal-to-ligand ratios when Na_3VO_4 and com-

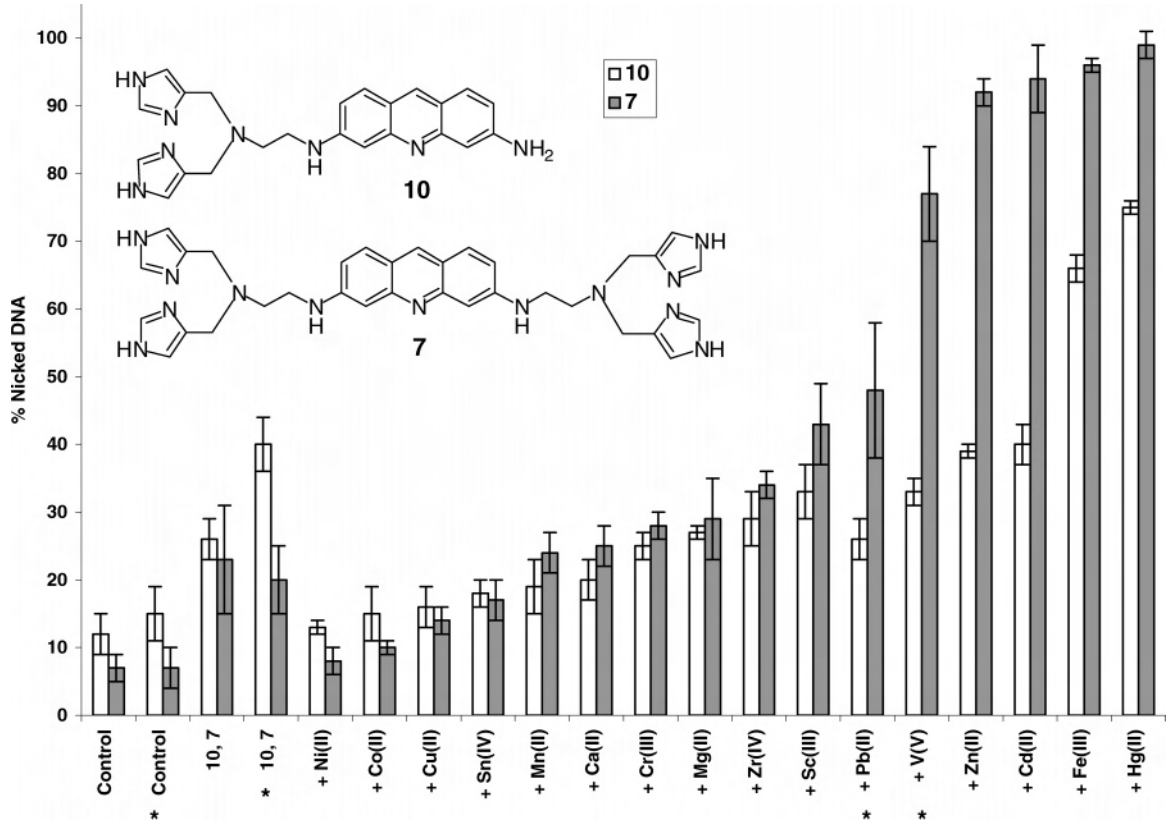

Figure 1. Histogram depicting metal-assisted photocleavage of pUC19 plasmid DNA in the presence of 50 μM **10** and 50 μM **7** without and with 25 μM metal salt as indicated (38 μM bp DNA, 20 mM sodium phosphate buffer pH 7.0). All reactions were irradiated with a broad-spectrum fluorescent lamp for 50 min at 22 °C. Percent cleavage (% nicked DNA) was averaged over three trials with error bars representing standard deviation. The asterisk identifies reactions in which 20 mM sodium cacodylate buffer pH 7.0 was used to substitute for sodium phosphate buffer. In the controls, DNA was irradiated in 20 mM buffer in the absence of **10**, **7**, and metal.

pound **7** were dissolved in a 1:1 ddH_2O:methanol solution. Taken together, the ESI mass spectral data indicate that the six metals undergo complexation in the order Cd(II) $\approx$ Zn(II) $>$ Hg(II) $\approx$ Pb(II) $\gg$ Fe(III) $>$ V(V).

Photocleavage Experiments. To determine the effects of various metals on DNA photocleavage, compounds **7** and **10** were individually treated in the presence of $CaCl_2 \cdot 2H_2O$, $CdCl_2$, $(CH_3)_2SnCl_2$, $CoCl_2 \cdot H_2O$, $CrCl_3 \cdot 6H_2O$, $CuCl_2 \cdot 2H_2O$, $FeCl_3 \cdot 6H_2O$, $HgCl_2$, $MgCl_2 \cdot 6H_2O$, $MnCl_2 \cdot 4H_2O$, Na_3VO_4, $NiCl_2 \cdot 6H_2O$, $PbCl_2$, $Sc(CF_3SO_3)_3$, $ZnCl_2$, and $ZrCl_4$. Photolysis reactions consisted of 20 mM sodium phosphate buffer pH 7.0 and 38 μM bp pUC19 plasmid DNA equilibrated in the absence and presence of 25 μM metal salt, 50 μM **7** or **10**, and 25 μM metal salt with 50 μM **7** or **10**.[13] (In reactions containing $PbCl_2$ and Na_3VO_4, 20 mM sodium cacodylate buffer pH 7.0 was used to substitute for sodium phosphate.) The samples were irradiated under aerobic conditions with a low-intensity, broad-spectrum 4 W T4T5/D fluorescent lamp for 50 min at 22 °C. After this, photocleavage products were resolved on a 1.0% nondenaturing agarose gel stained with ethidium bromide. ImageQuant Mac v. 1.2 software was then used to quantitate the % conversion of supercoiled plasmid DNA to its nicked form (Figure 1). This analysis revealed that DNA photocleavage by compound **7** was selectively enhanced in the presence of Hg(II), Fe(III), Cd(II), Zn(II), V(V), and Pb(II). In the case of compound **10**, Hg(II), Fe(III), Cd(II), and Zn(II) also increased photocleavage but at lower levels in comparison to **7**. (The fact that **7** possesses two additional imidazole rings may confer upon this compound superior metal-chelating ability.) As exemplified by the representative gel shown in Figure 2 (50 μM **7**, 25 μM $ZnCl_2$), minimal levels of photocleavage were always observed for DNA reactions irradiated in the absence of compound and metal (lane 1), in the absence of compound (lane 2), in the absence of metal (lane 3), and in a complete series of parallel reactions run in the dark (50 min, 22 °C; lanes 5−8). We therefore concluded that Hg(II), Fe(III), Cd(II), Zn(II), V(V), and Pb(II) ions could be used in combination with light to "tune" levels of DNA cleavage by compound **7**.

The central chromophore of compounds **7** and **10** is a DNA-binding 3,6-acridinediamine closely related in structure to acridine orange and proflavin (Figure S1 in the Supporting Information). It was therefore of interest to conduct a comparative analysis of DNA photocleavage. To accomplish this, individual reactions containing 50 μM acridine orange and proflavin without and with 25 μM $ZnCl_2$, 25 μM $FeCl_3$, and 200 μM imidazole were irradiated for 50 min with the broad-spectrum fluorescent lamp (38 μM bp pUC19 plasmid

(13) Optimal levels of DNA photocleavage were produced at a metal-to-ligand ratio of 1:2 for Hg(II), Cd(II), Zn(II), and Pb(II) and at a metal-to-ligand ratio of 2:1 for Fe(III) and V(V) (38 μM bp pUC19 plasmid DNA, 50 μM **7**). To facilitate comparison of the 16 metals, the experiments described in this paper were conducted using the 1:2 metal-to-ligand ratio.

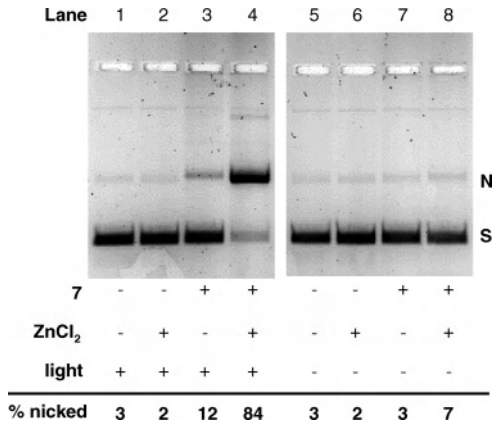

Figure 2. Photograph of a 1.0% nondenaturing agarose gel showing photocleavage of pUC19 plasmid DNA (50 μM **7** and 25 μM $ZnCl_2$ as indicated; 38 μM bp DNA; 20 mM sodium phosphate buffer pH 7.0; 22 °C). Lanes 1−4: reactions were irradiated with a broad-spectrum fluorescent lamp for 50 min. Lanes 5−8: parallel reactions maintained in the dark for 50 min. Abbreviations: N = nicked; S = supercoiled.

Table 1. Zn(II)- and Fe(III)-Assisted Photocleavage of pUC19 DNA by Acridine Orange, Proflavin, **7**, and **10**[a]

reactants	% nicked DNA			
	AO	P	**7**	**10**
DNA	14	14	7	12
DNA + 50 μM intercalator	28	15	23	26
DNA + 50 μM intercalator + 25 μM $ZnCl_2$	30	13	92	39
DNA + 50 μM intercalator + 25 mM $ZnCl_2$, 200 μM imidazole	35	11	NA	NA
DNA + 50 μM intercalator + 25 μM $FeCl_3$	29	15	96	66
DNA + 50 μM intercalator + 25 μM $FeCl_3$, 200 μM imidazole	27	17	NA	NA

[a] Photocleavage reactions consisted of 38 μM bp pUC19 plasmid DNA in sodium phosphate buffer pH 7.0 equilibrated without and with $ZnCl_2$, $FeCl_3$, imidazole, and the intercalators acridine orange, proflavin, **7**, and **10**. All reactions were irradiated with a broad-spectrum fluorescent lamp for 50 min at 22 °C. Abbreviations: AO = acridine orange; NA = not applicable; P = proflavin.

DNA, 20 mM sodium phosphate buffer pH 7.0, 22 °C). Yields were calculated and compared to data from the previous experiment (Table 1). It is evident that acridine orange, proflavin, **7**, and **10** all photocleave DNA at low levels in the absence of metal. However, upon the addition of either 25 μM $ZnCl_2$ or 25 μM $FeCl_3$, significant enhancements were observed for **7** and **10** but not in the case of acridine orange and proflavin. In an attempt to "mimic" the structure of compound **7**, 4 mol equiv of imidazole were added along with each metal salt to the acridine orange and proflavin reactions, but as shown in Table 1, levels of photocleavage were unaffected. It is apparent that metal-chelating imidazole must be covalently tethered to the DNA-binding 3,6-acridinediamine chromophore for Zn(II) and Fe(III) to enhance DNA photocleavage.

pH Profile. The Hg(II), Fe(III), Cd(II), Zn(II), V(V), and Pb(II)-assisted photocleavage reactions were then studied by means of an extensive pH profile in which 50 μM **7**, 25 μM metal salt, and 38 μM bp pUC19 plasmid DNA were irradiated in a variety of buffer systems: sodium cacodylate pH 5.0, 6.0, and 7.0; sodium phosphate pH 5.0, 6.0, 7.0, and 8.0; sodium borate pH 8.0 and 9.0 (Table 2). The goal of this experiment was to access the combined effects of buffer and pH to gain insight into possible mechanisms underlying metal-assisted DNA photocleavage.

At pH 5.0, compound **7** was shown to efficiently photocleave DNA in the absence of metal. However, as pH was raised, the general effect was to produce a decrease in photocleavage, irrespective of the buffer system employed (Table 2, first row). This result can be rationalized as follows. Compound **7** would be expected to bear a relatively high net positive charge at low pH and as a result would bind to negatively charged DNA with high affinity. However, at higher pH values, the positive charge on **7** would be reduced and as a result DNA binding affinity and photocleavage yields would decrease. Notwithstanding, it is evident that pH can be used as an additional chemical tool to "tune" the reactivity of compound **7**.

When **7** was reacted in the presence of Hg(II), Fe(III), Cd(II), Zn(II), V(V), and Pb(II), the greatest DNA photocleavage enhancement was observed at a pH value greater than 5.0 for each of the six metals (Table 2). It is conceivable that one or more of these metals might be compensating for the loss of positive charge experienced by compound **7** as pH is raised. (The effect of restoring electrostatic interactions between **7** and DNA would be to increase binding affinity and photocleavage yields.) The maximum cleavage enhancement was 85%, produced by Cd(II) in the presence of compound **7** and sodium phosphate buffer pH 8.0. This was followed by Zn(II), Cd(II), and Hg(II) ions, which increased DNA cleavage by 79% in sodium phosphate pH 6.0. At the near physiological pH value of 7.0, the best results were achieved by Hg(II) and Fe(III) in sodium phosphate buffer, which produced enhancements of 76% and 73%, respectively. This is significant for two reasons. The $H_2PO_4^-$ and HPO_4^{2-} conjugate pair constitutes one of the two most important buffering systems in human physiology. Second, iron, which is present in relatively high quantities in genomic DNA,[10] efficiently enhances DNA photocleavage in the phosphate buffer system. With respect to V(V) and Pb(II), the best photocleavage results were generally obtained by using sodium cacodylate buffer.

Intercalators and groove-binding compounds interact with double-helical DNA predominantly through $\pi-\pi$ stacking and a combination of van der Waals and electrostatic interactions, respectively. As a consequence, double-helical DNA is stabilized, increasing the melting temperature (T_m) of the duplex as a function of the binding affinity of the intercalator or groove binder. In an attempt to explain the trends observed in the above pH profile, thermal melting curves were used to determine T_m values of 12.5 μM bp calf thymus DNA in sodium phosphate buffer pH 5.0 and pH 7.0, in the absence and presence of 8 μM **7** (Figure 3). While compound **7** raised the T_m of calf thymus DNA from 65 to 94 °C at pH 5.0, the effect was much less pronounced at pH 7.0. In this case, the T_m was raised from 75 to 84 °C. In the absence of compound **7**, 4 μM $ZnCl_2$ had no effect on the melting temperature of the calf thymus DNA (T_m = 75 °C at pH 7.0). However, the addition of 4 μM $ZnCl_2$ to 8 μM **7** raised the T_m by 6 °C at pH 7.0, from 84 to 90 °C (Figure 3). Taken together, these data suggest that Zn(II) increases

Table 2. % DNA Photocleavage by Compound **7** as a Function of Buffer and pH[a]

	% nicked + % linear DNA								
reactants	pH 5.0 phosphate	pH 5.0 cacodylate	pH 6.0 phosphate	pH 6.0 cacodylate	pH 7.0 phosphate	pH 7.0 cacodylate	pH 8.0 phosphate	pH 8.0 borate	pH 9.0 borate
7	51 ± 8	64 ± 7	21 ± 7	28 ± 7	23 ± 8	20 ± 5	13 ± 5	19 ± 4	14 ± 4
7 + Hg(II)	97 ± 2 (46)	98 ± 1 (34)	100 ± 0 (79)	90 ± 1 (62)	99 ± 2 (76)	83 ± 3 (63)	81 ± 4 (68)	90 ± 3 (71)	80 ± 7 (66)
7 + Fe(III)	75 ± 3 (24)	96 ± 2 (32)	67 ± 6 (46)	95 ± 7 (67)	96 ± 1 (73)	83 ± 4 (63)	80 ± 4 (67)	64 ± 5 (45)	59 ± 11 (45)
7 + Cd(II)	96 ± 0 (45)	99 ± 1 (35)	92 ± 8 (79)	84 ± 5 (56)	94 ± 5 (71)	85 ± 4 (65)	98 ± 3 (85)	86 ± 6 (67)	74 ± 6 (60)
7 + Zn(II)	89 ± 2 (38)	92 ± 3 (28)	95 ± 5 (79)	83 ± 4 (55)	92 ± 2 (69)	66 ± 6 (46)	87 ± 4 (74)	71 ± 6 (52)	57 ± 6 (43)
7 + V(V)	93 ± 1 (42)	91 ± 4 (27)	83 ± 2 (62)	97 ± 3 (69)	56 ± 10 (33)	77 ± 7 (57)	22 ± 16 (9)	29 ± 11 (10)	9 ± 2 (−5)
7 + Pb(II)	22 ± 5 (−29)	87 ± 5 (23)	33 ± 8 (12)	95 ± 9 (67)	28 ± 2 (5)	48 ± 10 (28)	20 ± 9 (7)	61 ± 5 (42)	54 ± 6 (40)

[a] % DNA photocleavage = % nicked + % linear DNA. Listed in parentheses are % DNA photocleavage enhancement values expressed as the difference: % DNA photocleavage by **7** with metal minus % photocleavage by **7** without metal. Individual reactions consisted of 38 μM bp pUC19 plasmid DNA equilibrated with 50 μM **7**, 20 mM sodium phosphate, sodium cacodylate, or sodium borate buffers, without and with 25 μM metal salt (pH 5.0−9.0). All reactions were irradiated with a broad-spectrum fluorescent lamp for 50 min at 22 °C. The data are averaged over three trials, and errors are reported as standard deviation.

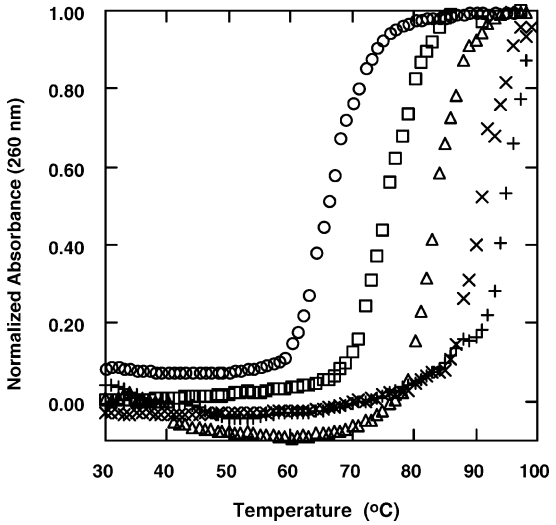

Figure 3. Effects of 8 μM compound **7**, 4 μM $ZnCl_2$, and 20 mM sodium phosphate buffers pH 5.0 and 7.0 on the thermal melting curve of 12.5 μM bp calf thymus DNA: ○, pH 5.0 buffer, T_m = 65 °C; □, pH 7.0 buffer, T_m = 75 °C; Δ, compound **7** in pH 7.0 buffer, T_m = 84 °C; ×, $ZnCl_2$ and compound **7** in pH 7.0 buffer, T_m = 90 °C; +, compound **7** in pH 5.0 buffer, T_m = 94 °C.

binding affinity and DNA photocleavage efficiency by restoring positive charge lost by **7** upon transition from pH 5.0 to 7.0.

Inhibition of DNA Photocleavage. Hydroxyl radical, hydrogen peroxide, singlet oxygen, and superoxide scavengers all reduce the formation of DNA strand breaks produced by the exposure of proflavin to visible light.[7b,c] A series of scavengers including the metal chelating agent ethylenediaminetetraacetic acid (EDTA) was therefore utilized to further investigate the mechanism(s) underlying metal-assisted DNA photocleavage by compound **7**. Individual photocleavage reactions consisted of 38 μM bp plasmid DNA in pH 7.0 buffer, 50 μM **7**, and 25 μM Hg(II), Fe(III), Cd(II), Zn(II), V(V), or Pb(II) in the presence of scavenger. Sodium azide was used to trap the type II reactive oxygen species (ROS) singlet oxygen ($^1O_2$), while superoxide dismutase (SOD), catalase, and sodium benzoate were employed for the type I ROS superoxide ($O_2^{\bullet -}$), hydrogen peroxide (H_2O_2), and hydroxyl radicals ($OH^{\bullet}$), respectively. The data in Table 3 show that EDTA consistently produced strong DNA photocleavage inhibition (≥78% in all cases). This result indicates that complexation between compound **7** and each

Table 3. % Inhibition of Metal-Assisted DNA Photocleavage[a]

metal	azide (100 mM)	benzoate (100 mM)	SOD (50 U)	catalase (50 U)	EDTA (100 mM)
Hg(II)	35 ± 6	2 ± 2	16 ± 6	24 ± 12	78 ± 7
Fe(III)	9 ± 6	20 ± 3	23 ± 12	66 ± 4	79 ± 4
Cd(II)	18 ± 3	7 ± 9	0 ± 1	26 ± 7	79 ± 8
Zn(II)	38 ± 13	28 ± 10	18 ± 7	35 ± 3	79 ± 6
V(V)	38 ± 10	38 ± 10	18 ± 9	41 ± 11	78 ± 7
Pb(II)	28 ± 8	32 ± 19	5 ± 4	53 ± 7	79 ± 2

[a] Individual reactions consisting of 38 μM bp pUC19 plasmid DNA, 50 μM **7**, 25 μM metal salt, and one of the above reagents were irradiated with a broad-spectrum fluorescent lamp for 50 min at 22 °C. The Zn(II), Cd(II), Hg(II), and Fe(III) reactions were in 20 mM sodium phosphate buffer pH 7.0 while the V(V) and Pb(II) reactions were in sodium cacodylate buffer pH 7.0. Percent inhibition was averaged over at least three trials with errors reported as standard deviation. Working reagent concentrations are in parentheses.

of the six metals is likely to be a prerequisite for efficient cleavage. In the Hg(II)/sodium benzoate, Fe(III)/sodium azide, Cd/sodium benzoate, Cd/SOD, and Pb(II)/SOD reactions, essentially no protection was observed. Otherwise, levels of photocleavage inhibition ranged from moderately low to high for all of the metal/scavenger combinations. (In the case of sodium benzoate, weak inhibitory effects cannot rule out the existence of nondiffusible hydroxyl radicals closely associated with the metal center of the complex. Second, because SOD produces H_2O_2 which itself can contribute to cleavage, weak inhibition by this enzyme cannot rule out superoxide.) In conclusion, the scavenger experiments collectively indicate that, with the exception of iron, type I and II photochemical processes are involved in compound **7** metal-assisted DNA cleavage. The Fe(III) reaction appears to proceed almost exclusively through a type I pathway.

Photocleavage at Lower Concentrations. Metal-assisted DNA photocleavage reactions were conducted using 8 μM **7**, 4 μM metal, and 12.5 μM bp pUC19 plasmid DNA. Because distortions in UV−visible and emission spectra are typically associated with highly concentrated chromophores, it was necessary for us to examine photocleavage patterns at these lower concentrations of **7** and metal to establish the feasibility of conducting additional spectroscopic studies. Reaction samples were irradiated with the broad-spectrum fluorescent lamp for 50 min at 22 °C. After this, the % conversion of supercoiled to nicked DNA produced by **7** in the presence of the 16 metal salts was quantitated. As shown

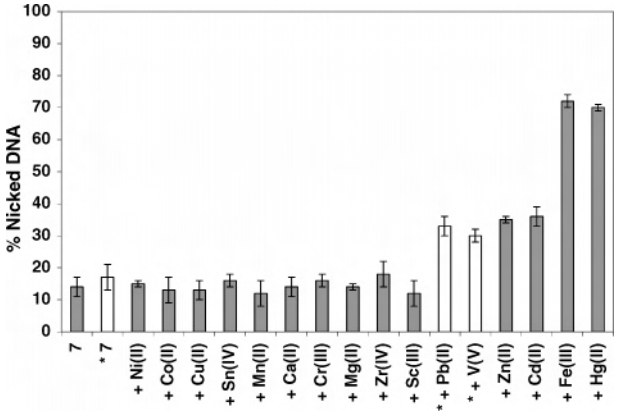

Figure 4. Histogram depicting metal-assisted photocleavage of pUC19 plasmid DNA in the presence of 8 μM **7** without and with 4 μM metal salt as indicated (12.5 μM bp DNA, 20 mM sodium phosphate buffer pH 7.0). All reactions were irradiated with a broad-spectrum fluorescent lamp for 50 min at 22 °C. Percent cleavage was averaged over three trials with error bars representing standard deviation. The asterisk identifies reactions in which 20 mM sodium cacodylate buffer pH 7.0 was used to substitute for sodium phosphate buffer.

in Figure 4, a similar trend was observed in the DNA photocleavage studies conducted at 50 μM **7** and 25 μM metal (Figure 1). The metal ions Hg(II), Fe(III), Cd(II), Zn(II), V(V), and Pb(II) all enhanced photocleavage at the lower reagent concentrations (Figure 4).

Absorbance and Emission Studies. In an attempt to account for the relative influence of the 16 metal salts on the efficiency of DNA photocleavage, we recorded absorbance and fluorescence emission spectra of compound **7** equilibrated in 20 mM sodium phosphate or in 20 mM sodium cacodylate pH 7.0 buffer, without and with metal salt (Table 4). We then calculated the % change in emission quantum yield resulting from the addition of each of the 16 metals to **7** (% $\Delta\Phi_{em}$ + metal) as well as the % change in absorbance intensity (% Δabs + DNA) and emission quantum yield (% $\Delta\Phi_{em}$ + DNA) and the change in the wavelength of maximum absorbance ($\Delta\lambda_{max}$ + DNA) resulting from the addition of calf thymus DNA (Table 4).

Bathochromic wavelength shifts and hypochromic absorption are characteristic of the electronic spectra of many DNA-bound groove binders and most if not all DNA-bound intercalators. The "% Δabs + DNA" and "$\Delta\lambda_{max}$ + DNA" data in Table 4 show that compound **7** demonstrates appreciable bathochromicity and hypochromicity in the presence of DNA. While the data cannot be used to account for different photocleavage levels, it is likely that compound **7** continues to bind to DNA in the presence of each of the 16 metals: red-shifts (positive "$\Delta\lambda_{max}$ + DNA" values) are consistently produced upon the addition of DNA, and with the exception of Ni(II), depressed absorption (negative "% Δabs + DNA") is observed. In addition, none of the metal-induced changes in the electronic spectra of **7** appear to be of sufficient magnitude to markedly attenuate or enhance levels of DNA photocleavage.

Upon binding to DNA, acridine orange exhibits an increase in fluorescence emission. In the case of proflavin, pronounced sequence dependent effects are seen. Fluorescence emission is increased in the presence of A·T-rich DNA but is almost completely quenched by G·C-rich sequences.[14] The "% $\Delta\Phi_{em}$ + DNA" values in Table 4 indicate that fluorescence is reduced upon the addition of DNA to (i) compound **7** and (ii) compound **7** in the presence of 15 out of 16 metals.

Table 4 also summarizes the effects of metal ions on compound **7** fluorescence emission in the absence of DNA. The 14 "% $\Delta\Phi_{em}$ + metal" values recorded in sodium phosphate buffer show that the photoinactive metals Ni(II), Cu(II), and Co(II) produce the most significant reductions in fluorescence intensity, followed by the three photoactive metals Hg(II), Cd(II), and Zn(II). The percent changes in emission quantum yield produced by the photoactive metal Fe(III) and the seven photoinactive metals Sn(IV), Sc(III), Zr(IV), Cr(III), Ca(II), Mg(II), and Mn(II) are all lower. Overall, the 14 metals follow the order Ni(II) > Cu(II) > Co(II) > Hg(II) > Cd(II) > Zn(II) > Fe(III) > Sn(IV) > Sc(III) = Zr(IV) > Cr(III) > Ca(II) > Mg(II) = Mn(II). The two "% $\Delta\Phi_{em}$ + metal" values recorded in sodium cacodylate buffer show that Pb(II) is a more efficient quencher than V(V).

According to hard−soft acid−base (HSAB) theory, the seven metals with the largest "% $\Delta\Phi_{em}$ + metal" values in their respective buffer systems are classified as either borderline or soft acids (Ni(II), Cu(II), Co(II), Hg(II), Cd(II), Zn(II), and Pb(II)), while the nine metals that have relatively minor effects on fluorescence emission (Fe(III), Sn(IV), Sc(III), Zr(IV), Cr(III), Ca(II), Mg(II), Mn(II), and V(V)), are classified as hard acids. Because imidazole is a borderline base, it is conceivable that compound **7** might display a preference for forming stable complexes with the seven borderline and soft metals. Therefore, it is possible that a relationship exists between the degree of fluorescence quenching and the degree of complex formation between compound **7** and each of the 16 metals.

Thermal Denaturation Studies. In our next set of experiments, we determined the T_m values of 12.5 μM bp calf thymus DNA at pH 7.0 in the absence and presence of 8 μM **7** and 4 μM of the 16 metal salts. The change in DNA melting temperature effected by the addition of metal to **7** was defined as $\Delta T_m = T_m$(**7** + metal) − T_m(**7**) (Table 4). Under our experimental conditions, the T_m obtained for calf thymus DNA was 74 ± 1 °C. The addition of each of the 16 metal salts to the DNA made little difference, since the resulting T_m values ranged from 73 to 75 °C. Therefore, none of the metals were able to effect the stability of double-helical calf thymus DNA on their own. Addition of **7** to the calf thymus DNA raised the T_m to 84 °C in 20 mM sodium phosphate buffer pH 7.0. When compound **7** and metals were present in combination, additional statistically significant increases in T_m were observed for 7 of the 16 metals: Ni(II), ΔT_m = 8 °C; Cd(II), ΔT_m = 6 °C; Zn(II), ΔT_m = 6 °C; Co(II), ΔT_m = 4 °C; Cu(II), ΔT_m = 3 °C; Hg(II), ΔT_m = 2 °C; Pb(II), ΔT_m = 2 °C. (T_m values determined over several trials showed the error in measurement to be ±1 °C.)

Taken together, the thermal denaturation and fluorescence quenching data suggest possible correlations between metal

(14) (a) Kubota, Y.; Steiner, R. F. *Biophys. Chem.* **1977**, *6*, 279−289. (b) Schreiber, J. P.; Daune, M. P. *J. Mol. Biol*. **1974**, *83*, 487−501.

Table 4. Absorbance, Emission, and Thermal Melting Data[a]

	absorbance studies				emission studies			T_m studies	
reactants	abs	% Δabs + DNA	λ_{max} (nm)	$\Delta\lambda_{max}$ + DNA	Φ_{em}	% $\Delta\Phi_{em}$ + metal	% $\Delta\Phi_{em}$ + DNA	T_m (°C)	ΔT_m (°C)
7	0.16	−6	459	8	0.090	NA	−26	84	NA
7 + Hg(II)	0.15	−10	451	16	0.025	−72	16	86	2
7 + Fe(III)	0.20	−21	459	8	0.068	−24	−28	84	0
7 + Cd(II)	0.18	−17	448	18	0.036	−60	−42	90	6
7 + Zn(II)	0.17	−17	458	9	0.062	−31	−42	90	6
7 + Sc(III)	0.21	−23	459	8	0.083	−8	−30	84	0
7 + Zr(IV)	0.21	−24	459	8	0.083	−8	−31	83	−1
7 + Mg(II)	0.21	−21	459	8	0.088	−2	−24	84	0
7 + Cr(III)	0.21	−18	458	9	0.085	−6	−22	83	−1
7 + Ca(II)	0.22	−29	459	8	0.087	−3	−18	84	0
7 + Mn(II)	0.20	−18	459	8	0.088	−2	−21	84	0
7 + Sn(IV)	0.22	−19	459	8	0.101	+12	−26	84	0
7 + Cu(II)	0.18	−19	452	7	0.019	−79	−74	87	3
7 + Co(II)	0.17	−15	448	11	0.023	−74	−74	88	4
7 + Ni(II)	0.12	3	448	16	0.011	−88	−46	92	8
***7**	0.16	−10	452	17	0.083	NA	−17	85	NA
***7** + V(V)	0.15	−27	451	20	0.080	−4	−12	86	1
***7** + Pb(II)	0.17	−24	452	18	0.074	−11	−40	87	2

[a] Absorbance and T_m measurements were conducted using solutions consisting of 8 μM **7** in 20 mM sodium phosphate buffer pH 7.0 equilibrated without and with 12.5 μM bp calf thymus DNA and 4 μM metal salt (22 °C). T_m data were averaged over two trials producing an average standard deviation of ±1 °C. Φ_{em} measurements were conducted at 25 °C with **7** in 20 mM sodium phosphate buffer pH 7.0 equilibrated without and with calf thymus DNA and metal salt. Absorbance in all Φ_{em} experiments was ~0.04 at the 430 nm excitation wavelength. Φ_{em} values were averaged over three trials producing an average standard deviation of ±0.002. Abbreviations: abs = absorbance intensity at λ_{max}; NA = not applicable; % Δ + DNA = percent change upon addition of DNA = [((**7** + metal + DNA) − (**7** + metal))/(**7** + metal)] × 100; Δ + DNA = change upon addition of DNA = (**7** + metal + DNA) − (**7** + metal); % Δ + metal = percent change upon addition of metal = [((**7** + metal) − (**7**))/(**7**)] × 100; $\Delta T_m = T_{m(7\ +\ metal)} - T_{m(7)}$. The asterisk identifies solutions in which 20 mM sodium cacodylate buffer pH 7.0 was used to substitute for 20 mM sodium phosphate buffer pH 7.0.

complex stability and DNA-binding affinity. The seven borderline and soft acids Ni(II), Cd(II), Zn(II), Co(II), Cu(II), Hg(II), and Pb(II) produce (i) appreciable positive ΔT_m values indicative of the formation of stable complexes that increase the binding affinity of **7** to DNA and (ii) moderate to high "% $\Delta\Phi_{em}$ + metal" values in their respective buffer systems. Alternatively, the nine hard metals Sn(IV), Mn(II), Ca(II), Cr(III), Mg(II), Zr(IV), Sc(III), V(V), and Fe(III) have no appreciable effects on T_m and have lower "% $\Delta\Phi_{em}$ + metal" values. Again, because imidazole is a borderline base, it is reasonable that compound **7** should display a preference for forming complexes with the seven borderline and soft metals rather than with the nine hard metals.

The appreciable ΔT_m values associated with Cd(II), Zn(II), Hg(II), and Pb(II) are consistent with the observation that levels of DNA photocleavage are increased when each of these four metals is added to compound **7** (Figures 1 and 4). In contrast, Ni(II), Co(II), and Cu(II) have appreciable ΔT_m values but at 25 μM concentrations yield the lowest levels of DNA photocleavage out of the 16 metals tested (Ni(II) < Co(II) < Cu(II); Figure 1). In addition, Ni(II), Co(II), and Cu(II) produce the three largest "% $\Delta\Phi_{em}$ + metal" values in Table 4 (Ni(II) > Cu(II) > Co(II)). In the case of many photosensitizers[5c] including the 3,6-acridinediamine proflavin,[7b,c,15] dye-sensitized generation of singlet oxygen ($^1O_2$; type II reaction) and superoxide ($O_2^{\bullet-}$; type I reaction) is thought to arise from the triplet state. With respect to compound **7**, fluorescence quenching by any one of the following three mechanisms could reduce the triplet state population, either directly or indirectly: (i) heavy atom or paramagnetically induced spin−orbit coupling that increases the rate of $S_1 \rightarrow T_1$ and $T_1 \rightarrow S_0$ processes; (ii) electron transfer between the excited singlet state fluorophore and the metal ion; (iii) energy transfer from the excited singlet state to the metal ion.[16] The efficiency of type I and II triplet state photochemical processes that contribute to DNA photocleavage would then be decreased. This hypothesis is consistent with the observations that compound **7** produces appreciably T_m values but extremely low levels of DNA photocleavage in the presence of Ni(II), Co(II), and Cu(II) (Figures 1 and 4). In a study of acridine orange−DNA−metal ternary complexes, Bregadze and co-workers observed significant emission quenching by Ni(II), Co(II), and Cu(II) relative to Mn(II) and Zn(II).[10] By calculating overlapping integrals and energy transfer radii, the investigators concluded that Ni(II), Co(II), and Cu(II) had quenched the excited singlet state of acridine orange by Förster-energy transfer.[10,17] While the photoactive metals Cd(II), Zn(II), Hg(II), and Pb(II) also produced relatively high levels of fluorescence quenching in our study, there is no reason to assume that any of the 16 metal ions we evaluated quench the singlet excited state of compound **7** by the same or even a single mechanism.

The two remaining metals in the series of 16 constitute a special case. As expected, the ΔT_m and "% $\Delta\Phi_{em}$ + metal" values of the hard acids V(V) and Fe(III) are negligible. However, DNA photocleavage by compound **7** is increased in both cases. For the six photoactive metals Hg(II), Fe(III),

(15) (a) van de Vorst, A.; Lion, Y. *Z. Naturforsch.* **1976**, *31*, 203−204. (b) van de Vorst, A.; Lion, Y.; Saucin, M. *Biochim. Biophys. Acta* **1976**, *430*, 467−477.

(16) (a) Prusik, T.; Kolubayev, T.; Morelli, M. J.; Brenner, H. C. *Photochem. Photobiol.* **1980**, *31*, 315−321. (b) Kemlo, J. A.; Shepherd, T. M. *Chem. Phys. Lett.* **1977**, *47*, 158−62. (c) Varnes, A. W.; Dodson, R. B.; Wehry, E. L. *J. Am. Chem. Soc.* **1972**, *94*, 946−950. (d) Lower, S. K.; El-Sayed, M. A. *Chem. Rev.* **1966**, *66*, 199−241. (e) McClure, D. S. *J. Chem. Phys.* **1952**, *20*, 682−686.

(17) Bregadze, V. G.; Chkhaberidze, J. G.; Khutsishvili, I. G. *Met. Ions Biol. Syst.* **1996**, *33*, 253−267.

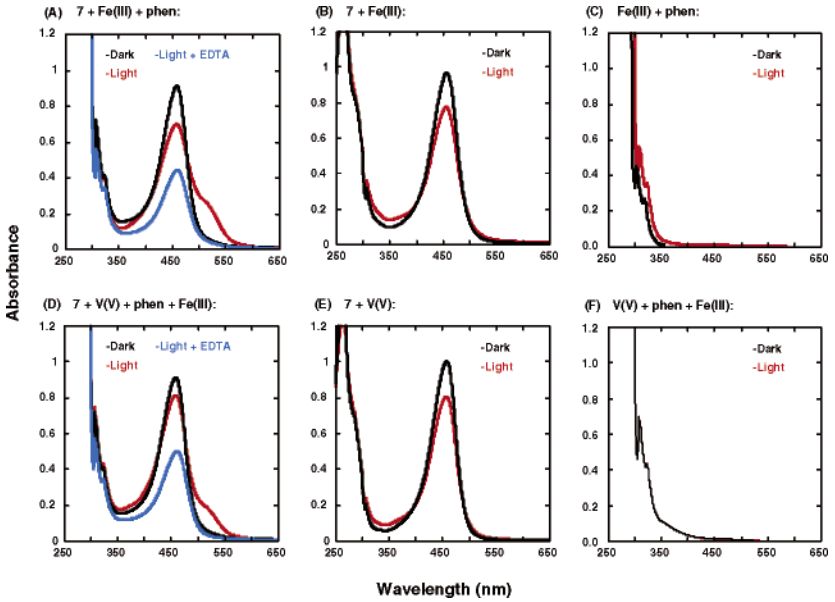

Figure 5. UV−visible spectra to detect Fe(II) (A−C) and V(IV) (D−F) formation in 20 mM pH 7.0 buffer. Reactions containing 25 μM $FeCl_3 \cdot 6H_2O$ or 25 μM Na_3VO_4, and 50 μM **7** and/or 400 μM 1,10-phenanthroline monohydrate were irradiated with a broad-spectrum visible lamp for 50 min at 22 °C (red) or were maintained in the dark for 50 min at 22 °C (black). A final concentration of 100 mM EDTA was added after irradiation (blue). In the V(IV) assay, 25 μM $FeCl_3 \cdot 6H_2O$ was added after irradiation (D, F).

Cd(II), Zn(II), V(V), and Pb(II), complex formation is indicated by scavenger experiments in which EDTA was shown to inhibit metal-assisted DNA photocleavage by **7** (Table 3). Additional evidence was provided by NMR and/or ESI mass spectra of **7** recorded in the presence of Hg(II), Fe(III), Cd(II), Zn(II), V(V), and Pb(II). While extensive 2:1 metal-to-ligand complex formation was observed only in the case of Cd(II) and Zn(II), 1:1 metallic complexes were formed by all six photoactive metals in the following order: Cd(II) ≈ Zn(II) > Hg(II) ≈ Pb(II) ≫ Fe(III) > V(V). Thus, the extent of metal complex formation was found to be in good agreement with the magnitude of the T_m increase: Cd(II) ≈ Zn(II) > Hg(II) ≈ Pb(II) ≫ Fe(III) ≈ V(V). Taken together, these data indicate that V(V) and Fe(III) are likely to form weak complexes with compound **7**. There is at least one reasonable explanation to account for the observation that both metals significantly enhance DNA photocleavage. It is well-known that electron transfer from the photochemically excited triplet states of acridine orange,[18a] proflavin,[18b] and other 3,6-acridinediamines[18b] effect photoreduction of Fe(III) to Fe(II). Although acridine-sensitized photoreduction of V(V) to V(IV) has not been documented, irradiation of oxoperoxovanadium(V) in acidic media has been shown to produce V(IV) with evolution of molecular oxygen.[19] A potential source of photocleavage enhancement might therefore involve compound **7**-sensitized one electron photoreduction of Fe(III) and V(V). The reduced metals would then be expected to produce highly reactive, DNA damaging hydroxyl radicals by the Fenton reaction.[20]

Spectrophotometric Determination of Fe(II) and V(IV). To test for photoreduction of Fe(III), we employed 1,10-phenanthroline, which forms a stable complex with Fe(II) (λ_{max} = 510 nm).[21] Because vanadium(IV) reduces ferric to ferrous ions, we then used a modified version of this colorimetric assay to detect V(IV).[22] For determination of Fe(II), individual photolysis reactions contained 20 mM sodium phosphate buffer pH 7.0 with two or more of the following reagents: 50 μM compound **7**; 25 μM $FeCl_3 \cdot 6H_2O$; 400 μM 1,10-phenanthroline monohydrate. The samples were then irradiated with the broad-spectrum fluorescent lamp (50 min at 22 °C), while a parallel set of reactions was kept in the dark. An irradiated reaction sample was then equilibrated in 100 mM EDTA to promote Fe(II)/1,10-phenanthroline complex disassociation. For V(IV) detection, the same procedure was employed except that (i) 20 mM sodium cacodylate buffer pH 7.0 and 25 μM Na_3VO_4 were used during photolysis to substitute for 20 mM sodium phosphate buffer and 25 μM $FeCl_3 \cdot 6H_2O$ and (ii) 25 μM $FeCl_3 \cdot 6H_2O$ was added immediately after the sample irradiation interval to enable V(IV) to reduce Fe(III) to Fe(II) and the Fe(II) product to form a complex with 1,10-phenanthroline. UV−visible spectra were immediately recorded (Figure 5).

The reaction irradiated in the presence of compound **7**, Fe(III), and 1,10-phenanthroline produced an orange color change and a ∼510 nm shoulder in the absorption band of **7** (Figure 5A). A similar shoulder appeared upon the addition of Fe(III) to the reaction irradiated in the presence of

(18) (a) Kellmann, A. *Photochem. Photobiol.* **1974**, *20*, 103−108. (b) Oster, G. K.; Oster, G. *J. Am. Chem. Soc.* **1959**, *81*, 5543−5545.
(19) Shinohara, N.; Nakamura, Y. *Bull. Chem. Soc. Jpn.* **1989**, *62*, 734−737.
(20) (a) Bandwar, R. P.; Rao, C. P. *J. Inorg. Biochem.* **1997**, *68*, 1−6. (b) Sakurai, H.; Tamura, H.; Okatani, K. *Biochem. Biophys. Res. Commun.* **1995**, *206*, 133−137. (c) Stohs, S. J.; Bagchi, D. *Free Radical Biol. Med.* **1995**, *18*, 321−336. (d) Shi, X.; Dalal, N. S. *Arch. Biochem. Biophys.* **1993**, *307*, 336−341. (e) Tullius, T. D.; Dombroski, B. A. *Proc. Natl. Acad. Sci. U.S.A.* **1986**, *83*, 5469−5473. (f) Halliwell, B.; Gutteridge, J. M. C. *Biochem. J.* **1984**, *219*, 1−14. (g) Fenton, H. J. H *J. Chem. Soc. Trans.* **1894**, *65*, 899−905.
(21) Bhat, R.; Hadi, S. M. *Mutagenesis* **1992**, *7*, 119−124.
(22) (a) Rao, G. N.; Prakash, R. *Curr. Sci.* **1974**, *43*, 279. (b) Vinkovetskaya, S. Y. *Nauchno. Tr. Nauchno.-Issled. Proekt. Inst. Redkometall. Prom.* **1973**, *42*, 202−204.

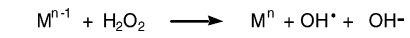

Figure 6. Fenton reaction. Abbreviation: M = metal.

compound **7**, V(V), and 1,10-phenanthroline (Figure 5D). When EDTA was added to both reactions, the 510 nm absorption became attenuated until the shoulder disappeared (Figure 5A,D). The signature orange color change and absorption at ~510 nm were absent in all of the dark reactions and in all of the reactions in which either 1,10-phenanthroline or compound **7** were omitted (Figure 5). These data collectively indicate that compound **7** sensitizes the one electron photoreduction of Fe(III) and V(V). There are numerous examples of stable Fe(II)[20c,e,g] and V(IV)[20a,b,d] complexes that participate in the Fenton reaction[20g] (Figure 6). The reduced metals react with hydrogen peroxide to produce short-lived, diffusible hydroxyl radicals ($OH^\bullet$) that cleave DNA with an extremely high rate constant. (In the case of iron, a few studies have suggested that a nondiffusible iron−oxygen (ferryl) radical is the active species formed.[20c,f]) Through the use of catalase, sodium benzoate, and superoxide dismutase, we showed that hydrogen peroxide (H_2O_2), hydroxyl radicals, and superoxide anion radicals ($O_2^{\bullet-}$) contribute to Fe(III)- and V(V)-assisted DNA photocleavage by compound **7** (Table 3). The H_2O_2 detected in these experiments was most likely formed through dismutation of superoxide anion radicals[20f] produced by type I electron transfer from the excited triplet state of compound **7** to O_2. The fact that the H_2O_2 was generated in the presence of Fe(II) and V(IV) suggests that the hydroxyl radicals we detected were from the Fenton reaction (Figure 6).

According to Rehm and Weller theory, excited-state redox potentials can be calculated from corresponding ground-state redox potentials and excited-state energies.[23] Thus, for acridine orange, the excited singlet state oxidation potential was estimated to be −1.71 V in 0.18 M phosphate buffer pH 6.5.[24] This value was obtained by Kittler and co-workers using eq 1, in which $U(^*D/D^{\bullet+})$ stands for excited-state oxidation potential, $U(D/D^{\bullet+})$ is the ground-state oxidation potential, and E_{oo} is excited-state energy.

$$U(^*D/D^{\bullet+}) = U(D/D^{\bullet+}) - E_{oo} \quad (1)$$

By substituting Kittler's value for the ground-state oxidation potential of acridine orange in 0.18 M phosphate buffer pH 6.5 (0.70 V)[24] and the excited triplet state energy of acridine orange (2.13 eV)[25] into eq 1, we obtained an estimated value of −1.43 V for the excited triplet state oxidation potential of acridine orange. Standard reduction potentials at pH 7.0 are 0.991[26] and −0.330 V[27] for the V(V)/V(IV) and $O_2/O_2^{\bullet-}$ couples, respectively. In the case of iron, the reduction potential of the LFe^{III}/LFe^{II} couple shows extreme variability on the basis of the nature of the ligand L: at pH 7.0, standard values range from −0.750 to 1.15 V.[28] Notwithstanding, the estimated excited singlet and excited triplet state oxidation potentials of acridine orange are more negative than all of the above ground-state reduction potentials, indicating that it should be possible for acridine orange to sensitize one electron reduction of V(V), Fe(III), and O_2. In the case of Fe(III) and O_2, this assertion is supported by the following experimental data. Acridine orange photosensitized cell inactivation[29] and proflavin triplet state photosensitized DNA cleavage[7b,15b] have both been associated with superoxide production, while the excited triplet states of acridine orange,[18a] proflavin,[18b] and other 3,6-acridinediamines[18b] have been shown to effect photoreduction of Fe(III) to Fe(II). Because the central core of compound **7** is a 3,6-acridinediamine nearly identical in structure with that of acridine orange (Figure S1 in the Supporting Information), the two chromophores are likely to have similar excited singlet and triplet state oxidation potentials. Electron transfer from the excited states of compound **7** to V(V), Fe(III), and O_2 should also be feasible. This hypothesis is consistent with the following lines of evidence reported in this paper. (i) In a series of scavenger experiments, SOD was shown to inhibit Hg(II)-, Fe(III)-, Zn(II)-, and V(V)-assisted DNA photocleavage, indicating that compound **7** is capable of photosensitizing one electron reduction of O_2 to $O_2^{\bullet-}$ (Table 3). (ii) In a spectrophotometric assay based on 1,10-phenanthroline, compound **7** was shown to photosensitize one electron reduction of Fe(III) and V(V) (Figure 5).

In summary, this report describes the synthesis and characterization of compounds **7** and **10**, which contain a central DNA binding 3,6-acridinediamine chromophore attached to 4 and 2 metal-coordinating imidazole rings, respectively. In a survey of 16 metal salts, we have demonstrated that the highest levels of DNA photocleavage are attained by **7** in the presence of either Hg(II), Fe(III), Cd(II), Zn(II), V(V), or Pb(II) (pH 7.0, 22 °C, 8−50 μM **7**). Scavenger experiments conducted with sodium azide, superoxide dismutase, catalase, and sodium benzoate indicated the involvement of type I and II photochemical processes in these metal-assisted DNA photocleavage reactions. Compound **7** afforded relatively low amounts of photocleavage both in the absence of metal and in the presence of either Ni(II), Co(II), Cu(II), Sn(IV), Mn(II), Ca(II), Cr(III), Mg(II), Zr(IV), or Sc(III). We also showed that photocleavage could be modulated by modifying buffer type and pH.

Metallic complex formation between compound **7** and the six photoactive metals Hg(II), Fe(III), Cd(II), Zn(II), V(V), and Pb(II) was implied by scavenger experiments in which EDTA was shown to inhibit metal-assisted DNA photocleavage. Direct evidence was provided by NMR and/or ESI mass spectral data.

On the basis of thermal melting and spectroscopic studies, we concluded that several phenomena were likely to influ-

(23) Rehm, D.; Weller, A. *Ber. Bunsen-Ges. Phys. Chem.* **1969**, *73*, 834−839.
(24) Kittler, L.; Loeber, G.; Gollmick, F. A.; Berg, H. *Bioelectrochem. Bioenerg.* **1980**, *7*, 503−511.
(25) Chambers, R. W.; Kearns, D. R. *Photochem. Photobiol.* **1969**, *10*, 215−219.
(26) Israel, Y.; Meites, L. In *Standard Potentials in Aqueous Solution*; Bard, A. J., Parsons, R., Jordan, J., Eds.; Marcel Dekker: New York, 1985; pp 507−525.
(27) Sawada, Y.; Iyanagi, T.; Yamazaki, I. *Biochemistry* **1975**, *14*, 3761−3764.
(28) Pierre, J. L.; Fontecave, M.; Crichton, R. R. *BioMetals* **2002**, *15*, 341−346.
(29) Martin J. P.; Logsdon, N. *Photochem. Photobiol.* **1987**, *46*, 45−53.

ence DNA photocleavage. When the 16 metals were added to **7**, significant changes in emission quantum yield and significant increases in T_m were observed only for the seven borderline and soft metals in the series. The ΔT_m values of 8 °C for Ni(II), 6 °C for Cd(II), 6 °C for Zn(II), 4 °C for Co(II), 3 °C for Cu(II), 2 °C for Hg(II), and 2 °C for Pb(II) indicate that the seven borderline and soft metals form complexes that increase the binding affinity of **7** to DNA. Alternatively, the minimal "% $\Delta\Phi_{em}$ + metal" and ΔT_m values associated with Fe(III), Sn(IV), Sc(III), Zr(IV), Cr(III), Ca(II), Mg(II), Mn(II), and V(V) suggest that that these nine hard metals are unable to form strong complexes with compound **7**. Regarding the six photoactive metals for which ESI mass spectra were recorded, the extent of metal complex formation (Cd(II) $\approx$ Zn(II) > Hg(II) $\approx$ Pb(II) $\gg$ Fe(III) > V(V)) was found to be in good agreement with the above melting temperature trends. It is likely that complex formation with positively charged metal enhanced electrostatic interactions between compound **7** and the negatively charged DNA phosphate backbone. This may in fact account for the increase in DNA photocleavage exhibited by compound **7** in the presence of Hg(II), Cd(II), Zn(II), and Pb(II). Although Ni(II), Co(II), and Cu(II) also raised the T_m when added to **7**, they were shown to efficiently quench fluorescence and in turn to inhibit photocleavage. Melting temperature values were unchanged upon addition of Fe(III) and V(V) to **7**, in agreement with fluorescence quenching data and with ESI spectra that showed weak complexation between the two metals and **7**. To account for the fact that DNA photocleavage was enhanced, we employed a colorimetric assay to demonstrate that compound **7** sensitized the one electron photoreduction of Fe(III) and V(V). The reduced metals would then accelerate the production of highly reactive, DNA damaging hydroxyl radicals by the Fenton reaction.[20]

Perhaps our most significant finding was the notable increase in compound **7** DNA photocleavage produced by Fe(III) in sodium phosphate buffer pH 7.0 (Figure 1, Figure 4, Table 2). This is important in light of the fact that the $H_2PO_4^-$ and HPO_4^{2-} conjugate pair constitutes one of the two most important buffering systems in human physiology. Second, iron is widely distributed throughout the human body and, as a result, has the potential to play an important role in the photodynamic action of compound **7** in vivo. Several lines of experimental evidence have established that cellular lysosomes contain low molecular weight pools of weakly chelated, redox active iron capable of catalyzing the Fenton reaction.[11,30] (This iron pool is thought to arise from lysosomal degradation of ferritin and other metalloproteins.) Upon entry into the cell, acridine orange accumulates mainly in the lysosomes and to the lesser degree in the cytoplasm and nucleus.[11,30a,c,31] After this, iron-catalyzed rupture of the lysosomal membranes is triggered by reactive oxygen species generated upon exposure to H_2O_2.[11,30a,c,32] Irradiation of acridine orange with intense blue light also produces reactive oxygen species that rupture the membranes.[31b,33] In both cases, the acridine orange is relocated from the lysosomes to the cytoplasm and nucleus.[11,30a,31b] It has recently been suggested that membrane rupture also triggers the diffusion of the weakly chelated iron from the lysosomes into the nucleus, resulting in significant damage to genomic DNA by the Fenton reaction.[11]

Acridine orange has demonstrated promise for use as a photosensitizer in photodynamic therapy. It is selectively localized in a number of tumor types and has been used to effect efficient in vivo photodestruction of epithelial tumors, Walker carcinosarcoma 256 stomach tumors, and musculoskeletal sarcomas in animal models.[8] Furthermore, the reactive oxygen species produced by irradiation of DNA bound acridine orange are thought to play a role in triggering tumor cell death.[8a,c,31a,34] The 3,6-acridinediamine **7** possesses four iron chelating imidazole rings attached to a central "acridine orange" core. In this paper, we have shown that iron markedly enhances DNA photocleavage by compound **7** in vitro, while having little if any effect on photocleavage produced by acridine orange (Table 1). We expect that it should also be possible for compound **7** to demonstrate superior photodynamic action in vivo. It is conceivable that compound **7** might chelate iron in lysosomes, facilitating the relocation of this metal to the nucleus upon irradiation-induced membrane rupture. Subsequent binding of **7** to nucleic acids would enable iron to catalyze the production of hydroxyl radicals within angstroms of genomic DNA.

Conclusions

Our data indicate that buffer, pH, Hg(II), Fe(III), Cd(II), Zn(II), V(V), Pb(II), and light can be used to "tune" DNA cleavage by compound **7** under physiologically relevant conditions. In addition to its potential use as a photosensitizer in photodynamic therapy, **7** has serendipitously demonstrated metal chemosensing capabilities as indicated by our spectrofluorometric experiments. Our immediate goal will be to explore the antitumor properties of compound **7** in vivo. The use of metal-coordinating imidazole rings may represent an attractive chemical tool to enhance the photodynamic action of acridine orange for chemotherapeutic purposes.

Experimental Section

General Methods. Melting points were determined in an Electrothermal IA9100 apparatus. Infrared spectra were taken on an FT-IR Perkin-Elmer 1725X spectrophotometer. All ^1H and ^{13}C

(30) (a) Persson, H. L.; Yu, Z.; Tirosh, O.; Eaton, J. W.; Brunk, U. T. *Free Radical Biol. Med.* **2003**, *34*, 1295−1305. (b) Yu, Z.; Persson, H. L.; Eaton, J. W.; Brunk, U. T. *Free Radical Biol. Med.* **2003**, *34*, 1243−1252. (c) Antunes, F.; Cadenas, E.; Brunk, U. T. *Biochem. J.* **2001**, *356*, 549−555. (d) Petrat, F.; De Groot, H.; Rauen, U. *Biochem. J.* **2001**, *356*, 61−69.

(31) (a) Kusuzaki, K.; Minami, G.; Takeshita, H.; Murata, H.; Hashiguchi, S.; Nozaki, T.; Ashihara, T.; Hirasawa, Y. *Jpn. J. Cancer Res.* **2000**, *91*, 439−445. (b) Brunk, U. T.; Dalen, H.; Roberg, K.; Hellquist, H. B. *Free Radical Biol. Med.* **1997**, *23*, 616−626.

(32) Hellquist, H. B.; Svensson, I.; Brunk, U. T. *Redox Rep.* **1997**, *3*, 65−70.

(33) (a) Zdolsek, J. M.; Olsson, G. M.; Brunk, U. T. *Photochem. Photobiol.* **1990**, *51*, 67−76. (b) Williams, D. S.; Slater, T. F. *Biochem. Soc. Trans.* **1973**, *1*, 200−202.

(34) Minami, G. *Kyoto-furitsu Ika Daigaku Zasshi* **1999**, *108*, 587−602.

NMR spectra were recorded at 300 and 75 MHz, respectively, on a Varian Mercury spectrometer. EI and CI mass spectra were generated on a Hewlett-Packard HP-5988a spectrometer at 70 eV, while ESI and APCI mass spectra were done either on an Automass Multi GC/API/MS Finnigan spectrometer or on a Micromass Q-Tof hybrid mass spectrometer. FAB mass spectra were recorded using a VG Autoexpec spectrometer with 3-nitrobenzyl alcohol as matrix. Elemental analyses were performed with a Heraeus CHN analyzer. Merck silica gel 60 (230−400 ASTM mesh) was employed for flash column chromatography. UV−visible spectra were recorded with a Shimadzu UV-1601 spectrophotometer, while a Cary Bio100 UV−vis spectrophotometer (Varian) was used to plot thermal melting curves.

Distilled, deionized water was utilized in the preparation of all buffers and aqueous reactions. Chemicals were of the highest available purity and were used without further purification. The metal salts $CaCl_2 \cdot 2H_2O$, $CdCl_2$, $(CH_3)_2SnCl_2$, $CoCl_2 \cdot H_2O$, $CrCl_3 \cdot 6H_2O$, $CuCl_2 \cdot 2H_2O$, $FeCl_3 \cdot 6H_2O$, $HgCl_2$, $MgCl_2 \cdot 6H_2O$, $MnCl_2 \cdot 4H_2O$, Na_3VO_4, $NiCl_2 \cdot 6H_2O$, $PbCl_2$, $Sc(CF_3SO_3)_3$, $ZnCl_2$, and $ZrCl_4$ were purchased from the Aldrich Chemical Co. (purity >99%). Superoxide dismutase and catalase were from Sigma. All other reagents, including cacodylic acid, ethidium bromide, 1,10-phenanthroline monohydrate, sodium azide, sodium benzoate, sodium borate, sodium cacodylate, sodium phosphate dibasic, and sodium phosphate monobasic, were from Aldrich. Both 1*H*-imidazole-4-methanol hydrochloride[35] and 4-(chloromethyl)-1*H*-imidazole hydrochloride[36] were synthesized according to reported procedures. Transformation of *Escherichia coli* competent cells (Stratagene, XL-1 blue) with pUC19 plasmid DNA (Sigma) and growth of bacterial cultures in Lauria-Bertani broth were performed using standard laboratory protocols.[37] The plasmid DNA was purified with a Qiagen Plasmid Mega Kit. Calf thymus DNA (average size of ≤2000 bp, Invitrogen Catalog No. 15633-019) was utilized without further purification.

To promote complex formation, aqueous stock solutions containing 250 μM of **7** or **10** and 125 μM of each respective metal salt were equilibrated in the dark for 24 h at 22 °C. Subsequent photocleavage experiments and absorbance, emission, and thermal melting studies were conducted using the equilibrated solutions diluted to the appropriate concentration.

2-[Bis(1*H*-imidazol-4-ylmethyl)amino]ethanol (1). To a solution of 2-aminoethanol (0.6 mL, 9.8 mmol) in dry ethanol (20 mL) was added triethylamine (5.5 mL, 39.2 mmol). The reaction mixture was heated at reflux after which a solution of 4-(chloromethyl)-1*H*-imidazole hydrochloride (3 g, 19.6 mmol) in dry ethanol (30 mL) was added dropwise over 20 min. The mixture was heated at reflux for 3 h and the solvent evaporated under reduced pressure. The resulting residue was stirred with dichloromethane (100 mL) for 2 h, from which an oil was separated. The dichloromethane was decanted and the oily product purified by flash column chromatography using silica gel as adsorbent and methanol−ethyl acetate (1:1) as eluent. This afforded **2** as a colorless oil in 70% yield. IR (KBr): 3108, 2879, 1628, 1571, 1450, 1085 cm^{-1}. ^1H NMR (CD_3OD): δ 7.76 (d, $J = 1.1$ Hz, 2H, H-2), 7.16 (d, $J = 1.1$ Hz, 2H, H-5), 3.88 (s, 4H, CH_2Im), 3.70 (t, $J = 5.5$ Hz, 2H, CH_2OH), 2.81 (t, $J = 5.5$ Hz, 2H, CH_2N). ^{13}C NMR (CD_3OD): δ 136.80 (C-2), 133.79 (C-4), 120.47 (C-5), 59.47 (CH_2OH), 55.70 (CH_2N), 50.23 (*C*H_2Im). MS (CI): *m*/*z* 222 ($[M + H]^+$, 32%), 170 (8), 161 (41), 142 (100), 109 (13), 90 (11), 81 (33). Anal. Calcd for $C_{10}H_{15}N_5O$: C, 54.28; H, 6.83; N, 31.65. Found: C, 54.04; H, 6.90; N, 31.91.

***N*-(2-Chloroethyl)-*N*-(1*H*-imidazol-4-ylmethyl)-1*H*-imidazole-4-methanamine Trihydrochloride (2).** To a solution of 2-[bis-(1*H*-imidazol-4-ylmethyl)amino]ethanol (**1**) (259 mg, 1.17 mmol) in dry DMF (5 mL) was added thionyl chloride (170 mL, 2.34 mmol). The reaction mixture was stirred at room temperature for 24 h and then concentrated to dryness. The oily product thus obtained was dissolved in methanol, precipitated with cold ethyl acetate, filtered out, and washed thoroughly with cold ethyl acetate. The hygroscopic solid was dried and kept under vacuum. Yield: 352 mg (86%). Mp: 173−174 °C. IR (KBr): 3412, 3118, 1701, 1621, 1439, 1277, 1169, 1087 cm^{-1}. ^1H NMR (CD_3OD): δ 8.92 (d, $J = 1.0$ Hz, 2H, H-2), 7.59 (d, $J = 1.0$ Hz, 2H, H-5), 3.96 (s, 4H, CH_2Im), 3.65 (t, $J = 6.5$ Hz, 2H, CH_2Cl), 2.93 (t, $J = 6.5$ Hz, 2H, CH_2N). ^{13}C NMR (CD_3OD): δ 135.63 (C-2), 131.43 (C-4), 119.22 (C-5), 55.80 (CH_2N), 48.45 (*C*H_2Im), 42.12 (CH_2Cl). MS (ESI): *m*/*z* 240 $[(M - 3HCl) + H]^+$ (calcd for $C_{10}H_{17}Cl_4N_5$: *m*/*z* 347). Anal. Calcd for $C_{10}H_{17}Cl_4N_5$: C, 34.58; H, 4.94; Cl, 40.31; N, 20.18. Found: C, 34.72; H, 4.91; N, 19.83.

***N*-(2-Chloroethyl)-*N*-[1-(triphenylmethyl)-1*H*-imidazol-4-ylmethyl]-1-(triphenylmethyl)-1*H*-imidazole-4-methanamine (3).** To a solution of *N*-(2-chloroethyl)-*N*-(1*H*-imidazol-4-ylmethyl)-1*H*-imidazole-4-methanamine trihydrochloride (**2**) (492 mg, 1.42 mmol) in dry DMF (8 mL) was added triethylamine (2 mL, 14.75 mmol). The reaction mixture was stirred at room temperature for 20 min, and then a solution of triphenylmethyl chloride (2.10 g, 7.36 mmol) in anhydrous DMF (20 mL) was added dropwise. After 2 h of stirring, the reaction mixture was poured onto crushed ice. The precipitate was filtered and purified by flash column chromatography using silica gel (0.1% Ca enriched) as adsorbent and ethyl acetate as eluent to give **3** in 61% yield. Mp: 125−127 °C. IR (KBr): 3059, 3031, 2927, 1596, 1492, 1444, 1324, 1237 cm^{-1}. ^1H NMR ($CDCl_3$): δ 7.36 (d, $J = 1.5$ Hz, 2H, H-2 Im), 7.30−7.26 (m, 18H, Ph), 7.13−7.08 (m, 12H, Ph), 6.60 (br s, 2H, H-5 Im), 3.64 (s, 4H, CH_2Im), 3.41 (t, $J = 7.4$ Hz, 2H, CH_2Cl), 2.84 (t, $J = 7.4$ Hz, 2H, CH_2N). ^{13}C NMR ($CDCl_3$): δ 142.36 (Cipso Ph), 138.48 (C-2 Im), 138.25 (C-4 Im), 129.65, 127.98, 127.92 (Ph), 120.43 (C-5 Im), 75.10 (CPh_3), 54.65 (CH_2N), 51.90 (CH_2Im), 42.13 (CH_2Cl). MS (APCI): *m*/*z* 724 ($[M + H]^+$) (calcd for $C_{48}H_{42}ClN_5$: *m*/*z* 723). Anal. Calcd for $C_{48}H_{42}ClN_5$: C, 79.63; H, 5.85; Cl, 4.83; N, 9.68. Found: C, 79.92; H, 5.62; N, 9.45.

3,6-Acridinediylbis(carbamic acid) Bis(1,1-dimethylethyl) Ester (4). To a solution of di-*tert*-butyl dicarbonate (26.4 mL, 115 mmol) in dry acetone (250 mL) was added 3,6-acridinediamine (2 g, 9.56 mmol). The reaction mixture was heated at reflux for 72 h and then concentrated to dryness. The crude product thus obtained was purified by flash column chromatography on silica gel using hexanes−ethyl acetate (1:1) as eluent. The 3,6-acridinediylbis-(carbamic acid) bis(1,1-dimethylethyl) ester (**4**) was obtained in 72% yield. Mp: >280 °C. IR (KBr): 3282, 2976, 1703, 1618, 1523, 1461, 1367, 1336, 1235, 1156 cm^{-1}. ^1H NMR (DMSO-d_6): δ 9.81 (s, 2H, N−H), 8.75 (s, 1H, H-9), 8.19 (d, $J = 2.2$ Hz, 2H, H-4, H-5), 7.96 (d, $J = 9.1$ Hz, 2H, H-1, H-8), 7.58 (dd, $J = 9.1$, 2.2 Hz, 2H, H-2, H-7), 1.52 (s, 18H, CMe_3). ^{13}C NMR (DMSO-d_6): δ 152.90 (CO), 149.95 (C-4a, C-10a), 141.39 (C-3, C-6), 135.26 (C-9), 129.18 (C-1, C-8), 122.01 (C-8a, C-9a), 119.67 (C-2, C-7), 112.40 (C-4, C-5), 79.88 (*C*Me_3), 28.29 (C*Me*$_3$). MS (EI): *m*/*z* 409 (M^+, 17%), 353 (8), 309 (18), 297 (93), 254 (13), 253 (83), 235 (3), 210 (11), 209 (72), 208 (25), 182 (31), 181 (37), 179

(35) Totter, J. R.; Darby, W. J. *Organic Syntheses*; Wiley & Sons: New York, 1955; Collect. Vol. III, pp 460−462.
(36) Turner, R. A.; Huebner, C. F.; Scholz, C. R. *J. Am. Chem. Soc.* **1949**, *71*, 2801−2803.
(37) Sambrook, J.; Fritsch, E. F.; Maniatis, T. In *Molecular Cloning A Laboratory Manual*, 2nd ed.; Cold Spring Harbor Press: New York, 1989.

(11), 154 (13), 153 (11), 127 (9). Anal. Calcd for $C_{23}H_{27}N_3O_4$: C, 67.46; H, 6.65; N, 10.26. Found: C, 67.59; H, 6.53; N, 10.02.

Continued elution with ethyl acetate and then with ethyl acetate−acetone−triethylamine (5:5:1) afforded the (6-amino-3-acridinyl)-carbamic acid 1,1-dimethylethyl ester (**8**) in 10% yield.

Synthesis of 3,6-Acridinediylbis[2-[bis[[1-(triphenylmethyl)-1*H*-imidazol-4-yl]methyl]amino]ethyl]carbamic Acid Bis(1,1-dimethylethyl) Ester (5). A mixture of 3,6-acridinediylbis(carbamic acid) bis(1,1-dimethylethyl) ester (**4**) (61 mg, 0.15 mmol) and Cs_2CO_3 (635 mg, 1.95 mmol) in dry DMF (5 mL) was stirred at room temperature for 30 min, after which a solution of *N*-(2-chloroethyl)-*N*-[1-(triphenylmethyl)-1*H*-imidazol-4-ylmethyl]-1-(triphenylmethyl)-1*H*-imidazole-4-methanamine (**3**) (225 mg, 0.31 mmol) in 5 mL DMF was added. After 24 h of stirring at room temperature, **3** (225 mg, 0.31 mmol) in 6 mL DMF was added. The reaction was stirred for another 24 h and then poured onto crushed ice. The resulting precipitate was collected, washed thoroughly with cold water, dried, and purified by flash column chromatography on silica gel using ethyl acetate−methanol (9:1) as eluent, yielding pure 3,6-acridinediylbis[2-[bis[[1-(triphenylmethyl)-1*H*-imidazol-4-yl]methyl]amino]ethyl]carbamic acid bis-(1,1-dimethylethyl) ester (**5**) (239 mg, 89%). Mp: 125−127 °C. IR (KBr): 3423, 3059, 2926, 2849, 1698, 1615, 1492, 1448, 1367, 1300, 1239, 1152, 1037 cm^{-1}. ^1H NMR ($CDCl_3$): δ 8.37 (s, 1H, H-9 Acr), 7.87 (d, $J = 1.8$ Hz, 2H, H-4, H-5 Acr), 7.62 (d, $J = 9.1$ Hz, 2H, H-1, H-8 Acr), 7.43 (dd, $J = 9.1$, 1.8 Hz, 2H, H-2, H-7 Acr), 7.31 (d, $J = 1.1$ Hz, 4H, H-2 Im), 7.23−7.15 (m, 36 H, Ph), 7.06−7.01 (m, 24 H, Ph), 6.49 (d, $J = 1.1$ Hz, 4H, H-5 Im), 3.92 (t, $J = 7.3$ Hz, 4H, CH_2N−Acr), 3.58 (s, 8H, CH_2Im), 2.84 (t, $J = 7.3$ Hz, 4H, CH_2N), 1.39 (s, 18H, CMe_3). ^{13}C NMR ($CDCl_3$): δ 154.15 (CO), 149.41 (C-4a, C-10a Acr), 144.81 (C-3, C-6 Acr), 142.41 (C_{ipso} Ph), 138.35 (C-2, C-4 Im), 134.62 (C-9 Acr), 129.63, 127.90, 127.83 (Ph), 127.49, (C-1, C-8 Acr), 126.97 (C-2, C-7 Acr), 124.31 (C-8a, C-9a Acr), 123.53 (C-4, C-5 Acr), 120.38 (C-5 Im), 80.56 (*C*Me_3), 74.97 (*C*Ph_3) 51.87 (CH_2N), 50.78 (*C*H_2Im), 48.53 (*C*H_2N−Acr), 28.35 (C*Me*$_3$). MS (FAB): *m*/*z* 1785, $[M + H]^+$ (calcd for $C_{119}H_{109}N_{13}O_4$: *m*/*z* 1784). Anal. Calcd for $C_{119}H_{109}N_{13}O_4$: C, 80.06; H, 6.15; N, 10.20. Found: C, 80.27; H, 6.22; N, 9.97.

3,6-Acridinediyl[2-[bis[[1-(triphenylmethyl)-1*H*-imidazol-4-yl]methyl]amino]ethyl]carbamic Acid Bis(1,1-dimethylethyl) Ester (6): mp 117−118 °C; IR (KBr) 3415, 3058, 2975, 1698, 1617, 1569, 1544, 1492, 1450, 1367, 1240, 1152, 1037 cm^{-1}; ^1H NMR ($CDCl_3$) δ 8.46 (s, 1H, H-9 Acr), 7.92 (d, $J = 1.7$ Hz, 1H, H-4 Acr), 7.87 (br s 2H, H-7, H-8 Acr), 7.76 (br s, H-5 Acr), 7.64 (d, $J = 8.9$ Hz, 1H, H-1 Acr), 7.41 (dd, $J = 8.9$, 1.7 Hz, H-2 Acr), 7.31 (d, $J = 1.3$ Hz, 2H, H-2 Im), 7.23−7.20 (m, 18H Ph), 7.05−7.02 (m, 12H, Ph), 6.52 (d, $J = 1.3$ Hz, 2H, H-5 Im), 3.90 (t, $J = 7.0$ Hz, 4H, CH_2N−Acr), 3.59 (s, 4H, CH_2Im), 2.84 (t, $J = 7.0$ Hz, 2H, CH_2N), 1.58 (s, 9H, CMe_3), 1.39 (s, 9H, CMe_3); ^{13}C NMR ($CDCl_3$) δ 154.12, 152.40 (CO) 149.55 (C-4a, C-10a Acr), 144.97 (C-3, C-6 Acr), 142.42 (C_{ipso} Ph), 138.35 (C-2, C-4 Im), 135.01 (C-9 Acr), 129.64 (C-8 Acr and Ph), 127.88 (Ph), 127.80 (Ph and C-1 Acr), 126.57 (C-2 Acr), 123.78 (C-8a Acr), 123.25 (C-9a, C-4a Acr), 120.42 (C-5 Im), 119.78 (C-7 Acr), 113.70 (C-5 Acr), 81.12, 80.60 (*C*Me_3), 75.01 (*C*Ph_3), 51.78 (CH_2N), 50.94 (*C*H_2Im), 48.42 (*C*H_2N−Acr), 28.32 (C*Me*$_3$); MS (FAB) *m*/*z* 1097, $[M + H]^+$ (calcd for $C_{71}H_{68}N_8O_4$: *m*/*z* 1096). Anal. Calcd for $C_{71}H_{68}N_8O_4$: C, 77.71; H, 6.25; N, 10.21. Found: C, 77.51; H, 6.34; N, 10.47.

***N,N′*-Bis[2-[bis(1*H*-imidazol-4-ylmethyl)amino]ethyl]-3,6-acridinediamine (7).** A suspension of **5** (591 mg, 0.33 mmol) in 2 N HCl (20 mL) was heated at 50−60 °C for 3.5 h. The resulting precipitate of triphenylmethanol was filtered off and the filtrate basified to pH 8−9 with 2 N NaOH. The precipitate thus obtained was filtered out, washed with cold water, and dried in a vacuum desiccator to give 177 mg (87%) of pure product. Mp: 146−148 °C. IR (KBr): 3118, 2923, 2834, 2834, 1642, 1610, 1450, 1375, 1279, 1168, 1105 cm^{-1}. ^1H NMR (CD_3OD): δ 8.30 (s, 1H, H-9 Acr), 7.62−7.58 (m, 6H, H-1, H-8 Acr and H-2 Im), 6.97 (d, 4H, $J = 0.7$ Hz, 4H, H-5 Im), 6.90 (dd, $J = 9.2$, 2.2 Hz, 2H, H-2, H-7 Acr), 6.58 (d, $J = 2.2$ Hz, 2H, H-4, H-5 Acr), 3.69 (s, 8H, CH_2Im), 3.28 (t, $J = 5.9$ Hz, 4H, CH_2N−Acr), 2.76 (t, $J = 5.9$ Hz, 4H, CH_2N). ^{13}C NMR (CD_3OD): δ 153.13 (C-4a, C-10a Acr), 150.36 (C-3, C-6 Acr), 138.54 (C-9 Acr), 136.49 (C-2 Im), 134.90 (C-4 Im), 130.64 (C-1, C-8 Acr), 120.65 (C-5 Im), 120.10 (C-8a, C-9a Acr), 119.22 (C-2, C-7 Acr), 97.91 (C-4, C-5 Acr), 52.13 (CH_2N), 50.74 (*C*H_2Im), 41.72 (*C*H_2N−Acr). MS (FAB): *m*/*z* 616, $[M + H]^+$ (calcd for $C_{33}H_{37}N_{13}$: *m*/*z* 615). Anal. Calcd for $C_{33}H_{37}N_{13}$: C, 64.37; H, 6.06; N, 29.57. Found: C, 64.24; H, 6.11; N, 29.71.

(6-Amino-3-acridinyl)carbamic Acid 1,1-Dimethylethyl Ester (8). To a solution of di-*tert*-butyl dicarbonate (4.4 mL, 19.12 mmol) in dry acetone (150 mL) was added 3,6-acridinediamine (2 g, 9.56 mmol). The reaction mixture was heated at reflux for 8 h and then concentrated to dryness. The crude product thus obtained was purified by flash column chromatography using silica gel as adsorbent. With hexanes−ethyl acetate (1:1) as eluent, 3,6-acridinediylbis(carbamic acid) bis(1,1-dimethylethyl) ester **(4)** (746 mg, 25%) was obtained. Continued elution with ethyl acetate and then ethyl acetate−acetone−triethylamine (5:5:1) afforded 2.3 g (59%) of the (6-amino-3-acridinyl)carbamic acid 1,1-dimethylethyl ester **(8)**. Mp: >280 °C. IR (KBr): 3363, 2976, 1709, 1624, 1572 cm^{-1}. ^1H NMR (DMSO-d_6): δ 9.69 (s, 1H, N−H), 8.50 (s, 1H, H-9), 8.05 (d, $J = 2.1$ Hz, 1H, H-4), 7.81 (d, $J = 9.1$ Hz, 1H, H-1), 7.73 (d, $J = 9.1$ Hz, 1H, H-8), 7.43 (dd, $J = 9.1$, 2.1 Hz, 1H, H-2), 6.99 (dd, $J = 9.1$, 2.1 Hz, 1H, H-7), 6.85 (d, $J = 2.1$ Hz, 1H, H-5), 6.04 (s, 2H, NH_2), 1.51 (s, 9H, CMe_3). ^{13}C NMR (DMSO-d_6): δ 152.93 (CO), 151.49 (C-10a), 151.06 (C-6), 49.75 (C-4a), 140.93 (C-3), 134.96 (C-9), 129.61 (C-8), 129.12 (C-1), 120.54 (C-9a), 120.11 (C-8a), 120.00 (C-7), 117.68 (C-2), 112.16 (C-4), 102.93 (C-5), 79.68 (*C*Me_3), 28.32 (C*Me*$_3$). MS (EI): *m*/*z* 309 (M^+, 8%), 253 (33), 235 (23), 209 (100), 182 (31), 181 (25), 127 (5), 104 (7), 57 (10). Anal. Calcd for $C_{18}H_{19}N_3O_2$: C, 69.88; H, 6.19; N, 13.58. Found: C, 69.61; H, 6.13; N, 13.84.

(6-Amino-3-acridinyl)[2-[bis[[1-(triphenylmethyl)-1*H*-imidazol-4-yl]methyl]amino]ethyl]carbamic Acid 1,1-Dimethylethyl Ester (9). To a mixture of 6-amino-3-acridinyl)carbamic acid 1,1-dimethylethyl ester (**8**) (156 mg, 0.51 mmol) and cesium carbonate (900 mg, 2.76 mmol) in dry DMF (40 mL) was added *N*-(2-chloroethyl)-*N*-[1-(triphenylmethyl)-1*H*-imidazol-4-ylmethyl]-1-(triphenylmethyl)-1*H*-imidazole-4-methanamine (**3**) (400 mg, 0.55 mmol). The reaction mixture was stirred at room temperature under argon. After 24 and 48 h, an additional amount (100 mg, 0.14 mmol) of **3** was added. Finally, the reaction was stirred for another 24 h and then poured onto crushed ice. The precipitate was filtered out and washed with cold water. The solid thus obtained was purified by column chromatography on silica gel (0.1% Ca enriched) using ethyl acetate−triethylamine (10:1) and acetone−ethyl acetate−triethylamine (5:5:1) as eluents, yielding pure **9** (428 mg, 85%). Mp: 115−117 °C. IR (KBr): 3353, 3058, 2925, 1694, 1641, 1612, 1492, 1463, 1445 cm^{-1}. ^1H NMR (CD_3OD): δ 8.46 (s, 1H, H-9 Acr), 7.77 (d, $J = 9.0$, 1H, H-8 Acr), 7.71 (d, $J = 2.0$, 1H, H-4 Acr), 7.61 (d, $J = 9.0$ Hz, 1H, H-1 Acr), 7.29 (d, $J = 1.5$ Hz, 2H, H-2 Im), 7.21−7.18 (m, 19H, H-2 Acr and Ph), 7.12 (dd, $J = 9.0$, 2.0 Hz, 1H, H-7 Acr), 7.01−6.96 (m, 13H, H-5 Acr and Ph), 6.55 (d, $J = 1.5$ Hz, 2H, H-5 Im), 3.82 (t, $J = 7.0$ Hz, 2H, CH_2N−Acr), 3.52 (s, 4H, CH_2Im), 2.74 (t, $J = 7.0$ Hz, 2H, CH_2N), 1.36

(s, 9H, CMe_3). ^{13}C NMR (CD_3OD): δ 155.52 (CO), 153.43 (C-10a Acr), 151.69 (C-4a Acr), 148.94 (C-6 Acr), 146.14 (C-3 Acr), 143.28 (C_{ipso} Ph), 139.01, 138.88 (C-2, C-4 Im), 137.84 (C-9 Acr), 130.89 (C-8 Acr), 130.49 (Ph), 129.62 (C-1 Acr), 129.02 (Ph), 125.31 (C-2 Acr), 123.35, 122.89, (C-8a, C-9a Acr), 122.28 (C-4 Acr), 121.89, 121.82 (C-5 Im, C-7 Acr), 102.54 (C-5 Acr), 82.00 (CMe_3), 76.64 (CPh_3), 54.79 (CH_2N), 52.72 (CH_2Im), 52.18 (CH_2N-Acr), 28.71 (CMe_3). MS (FAB): *m*/*z* 997, $[M + H]^+$ (calcd for $C_{66}H_{60}N_8O_2$: *m*/*z* 996). Anal. Calcd for $C_{66}H_{60}N_8O_2$: C, 79.49; H, 6.06; N, 11.24. Found: C, 79.63; H, 6.21; N, 10.96.

***N*-[2-[Bis(1*H*-imidazol-4-ylmethyl)amino]ethyl]-3,6-acridinediamine (10).** A suspension of **9** (377 mg, 0.38 mmol) in 2 N HCl (20 mL) was heated at 50−60 °C for 3.5 h. The resulting white precipitate of triphenylmethanol was filtered off and the filtrate basified to pH 8−9 with 2 N NaOH. The precipitate thus obtained was filtered and dried in a vacuum desiccator, affording 109 mg (70%) of pure product that decomposed above 198 °C. IR (KBr): 3328, 3115, 2827, 1610, 1521, 1464, 1418, 1390, 1274, 1223, 1159, 1104 cm-1. ^1H NMR (CD_3OD): δ 8.36 (s, 1H, H-9 Acr), 7.67−7.60 (m, 2H, H-1, H-8 Acr), 7.63 (s, 2H, H-2 Im), 7.25 (s, 1H, NH−Acr), 6.97 (s, 2H, H-5 Im), 6.91 (m, 2H, H-2, H-7 Acr), 6.85 (br s, 1H, H-5 Acr), 6.58 (br s, 1H, H-4 Acr), 3.68 (s, 4H, CH_2Im), 3.27 (t, J = 6.0 Hz, 2H, CH_2N-Acr), 2.74 (t, J = 6.0 Hz, 2H, CH_2N). ^{13}C NMR (CD_3OD): δ 153.80, 153.33, (C-4a, C-10a Acr), 150.24, 149.76, (C-3, C-6 Acr), 139.02 (C-9 Acr), 136.49 (C-2 Im), 134.99 (C-4 Im), 131.30, 130.78, (C-1, C-8 Acr), 120.60 (C-5 Im), 120.11, 119.94, (C-8a, C-9a Acr), 119.44, 118.87 (C-2, C-7 Acr), 101.50 (C-5 Acr), 97.46 (C-4 Acr), 52.09 (CH_2N), 50.74 (CH_2-Im), 41.69 (CH_2N-Acr). MS (FAB): *m*/*z* 413, $[M + H]^+$ (calcd for $C_{23}H_{24}N_8$: *m*/*z* 412). Anal. Calcd for $C_{23}H_{24}N_8$: C, 66.97; H, 5.86; N, 27.16. Found: C, 66.84; H, 5.61; N, 27.56.

Photocleavage Experiments. In a total volume of 20 μL, individual reactions contained 38 μM bp pUC19 plasmid DNA in (i) 20 mM buffer or in (ii) 20 mM buffer, 50 μM **7**, and/or 25 μM of one of the following metal salts: $CaCl_2 \cdot 2H_2O$, $CdCl_2$, $(CH_3)_2SnCl_2$, $CoCl_2 \cdot H_2O$, $CrCl_3 \cdot 6H_2O$, $CuCl_2 \cdot 2H_2O$, $FeCl_3 \cdot 6H_2O$, $HgCl_2$, $MgCl_2 \cdot 6H_2O$, $MnCl_2 \cdot 4H_2O$, Na_3VO_4, $NiCl_2 \cdot 6H_2O$, $PbCl_2$, $Sc(CF_3SO_3)_3$, $ZnCl_2$, or $ZrCl_4$. The buffer systems employed were the following: 20 mM sodium cacodylate pH 5.0, 6.0, and 7.0; 20 mM sodium phosphate pH 5.0, 6.0, 7.0, and 8.0; sodium borate pH 8.0 and 9.0. Reactions were kept in the dark or were irradiated for 50 min at 22 °C in 1.7 mL microcentrifuge tubes with a broad-spectrum 4 W T4T5/D fluorescent lamp (EIKO Ltd.) located 6 cm above the opened tubes. Aerobic ventilation was achieved by placing a table fan directly adjacent to the lamp. Cleavage products were then electrophoresed on a 1.0% nondenaturing agarose gel stained with ethidium bromide (0.5 μg/mL), visualized on a transilluminator set at 302 nm, photographed, and scanned. Amounts of supercoiled, nicked, and linear plasmid DNA were then quantitated using ImageQuant Mac v. 1.2 software (Amersham Biosciences). In the calculation of photocleavage yields, the density of the supercoiled DNA band was multiplied by a correction factor of 1.22 to compensate for the relatively low ethidium bromide staining efficiency of supercoiled DNA compared to nicked and linear plasmid.

Thermal Melting Studies. Individual 3 mL solutions containing 12.5 μM bp calf thymus DNA in (i) 20 mM sodium phosphate buffer pH 7.0 or in (ii) 20 mM sodium phosphate buffer pH 7.0, 8 μM **7**, and/or 4 μM of each of the 16 metal salts were placed in 3 mL (1 cm) quartz cuvettes (Starna). For V(V) and Pb(II), 20 mM sodium cacodylate buffer was used to substitute for the sodium phosphate buffer. While absorbance was monitored at 260 nm, DNA was denatured by using a Peltier heat block to increase the temperature from 25 to 100 °C at a rate of 0.5 °C min^{-1}. KaleidaGraph version 3.5 was then utilized to approximate the first derivative of $\Delta A_{260}/\Delta T$ vs temperature, where the T_m value at the inflection point of each sigmoidal melting transition was marked by the maximum of its corresponding first derivative plot.

Scavenger Experiments. Individual 20 μL reactions containing 20 mM sodium phosphate buffer pH 7.0, 38 μM bp pUC19 plasmid DNA, 50 μM **7**, and 25 μM of the metal salts $CdCl_2$, $FeCl_3 \cdot 6H_2O$, $HgCl_2$, Na_3VO_4, $PbCl_2$, and $ZnCl_2$ were irradiated with a broad-spectrum 4 W T4T5/D fluorescent lamp (EIKO Ltd.) in the presence of either 100 mM sodium azide, 100 mM sodium benzoate, 50 U superoxide dismutase, 50 U catalase, or 100 mM EDTA (50 min at 22 °C). For V(V) and Pb(II), 20 mM sodium cacodylate buffer was used to substitute for the sodium phosphate buffer. Reaction products were then resolved on a 1.0% nondenaturing agarose gel and quantitated as described above. The percent inhibition of DNA photocleavage was calculated on the basis of cleavage yields obtained in parallel reactions run without scavenger: [((% cleavage in the presence of **7** and metal) − (% cleavage in the presence of scavenger, **7**, and metal))/(% cleavage in the presence of **7** and metal)] × 100.

Quantum Yield Measurements. Emission spectra were recorded from 440 to 630 nm at 25 °C in 1 cm quartz cuvettes (Starna) using an Olis SLM-8000 spectrofluorimeter equipped with Olis Spectral Works v. 3.0.12 software. A 2 μM solution of proflavin in 50 mM potassium acetate buffer pH 4.0 (Φ = 0.27,[38] λ_{max} = 444 nm, ϵ = 30 800 M^{-1} cm^{-1}) was used as the reference to calculate the quantum yields of 5 μM **7** in 20 mM sodium phosphate buffer pH 7.0 (λ_{max} = 459 nm, ϵ = 20 000 M^{-1} cm^{-1}) and in 20 mM sodium cacodylate buffer pH 7.0. Compound **7**, calf thymus DNA, and metal salt were adjusted to the following concentrations to give an absorbance of ∼0.04 at the 430 nm excitation wavelength: 4−7 μM **7** and 2−3.5 μM metal salt in solutions containing compound **7** and metal salt; 7−10 μM **7**, 3.5−5 μM metal salt, and 10.9−15.6 μM bp DNA in solutions containing compound **7**, metal salt, and calf thymus DNA. Additional emission spectra were then recorded in 20 mM sodium phosphate pH 7.0 and in 20 mM sodium cacodylate pH 7.0 after which emission quantum yields were determined relative to **7** in the appropriate buffer. The excitation and emission monochromator slit widths of the spectrofluorimeter were set at 1 and 8 nm, respectively. An excitation polarizer set at 0° and an emission polarizer set at the "magic angle" (54.7°) were used to eliminate possible effects from nonisotropic fluorescence. Lamp spectral intensity output was monitored by recording the Raman peak of water (λ_{ex} = 350 nm, λ_{em} 397 nm) and the emission of **7** (λ_{ex} = 430 nm, λ_{em} = 500 nm). The emission spectra were corrected for wavelength-dependent response of the spectrofluorimeter, converted to quanta units, and integrated. Relative emission quantum yields were then calculated by the comparative method.[39] All data were averaged over three trials with errors reported as standard deviation.

Colorimetric Detection of Fe(II).[21] A series of 500 μL reactions was prepared containing 20 mM sodium phosphate buffer pH 7.0 and two or more of the following reagents: 50 μM **7**; 25 μM $FeCl_3 \cdot 6H_2O$; 400 μM 1,10-phenanthroline monohydrate. The samples were irradiated with the 4W F4T5/D fluorescent lamp, while a parallel set of reactions was kept in the dark. After 50 min, the solutions were visually examined for color change and placed in 500 μL quartz cuvettes, and absorbance was monitored between

(38) Melhuish, W. H. *J. Opt. Soc. Am.* **1964**, *54*, 183−186.
(39) (a) Fery-Forgues, S.; Lavabre, D. *J. Chem. Educ.* **1999**, *76*, 1260−1264. (b) Demas, J. N.; Crosby, G. A. *J. Phys. Chem.* **1971**, *75*, 991−1024. (c) Parker, C. A.; Rees, W. T. *Analyst* **1960**, *85*, 587−600.

250 and 650 nm for evidence of Fe(II)−1,10-phenanthroline complex formation. To dissociate the 510 nm complex, an irradiated reaction containing 50 μM **7**, 25 μM $FeCl_3 \cdot 6H_2O$, and 400 μM 1,10-phenanthroline was equilibrated in 100 mM EDTA for 6 h in the dark.

Colorimetric Detection of V(IV).[22] To detect V(IV), the following modifications were made to the colorimetric assay described above. (i) A 20 mM sodium cacodylate buffer (pH 7.0) and 25 μM Na_3VO_4 were used during photolysis to substitute for 20 mM sodium phosphate buffer and 25 μM $FeCl_3 \cdot 6H_2O$. (ii) After 50 min of irradiation, 12.5 μL of 1 mM $FeCl_3 \cdot 6H_2O$ was added to the reactions containing **7**, V(V), and 1,10-phenanthroline and V(V) and 1,10-phenanthroline. The solutions were equilibrated in the dark for 45 min, visually examined for color change, and monitored between 200 and 650 nm for evidence of Fe(II)−1,10-phenanthroline complex formation.

Acknowledgment. We thank Professors Thomas L. Netzel and Markus W. Germann (Georgia State University) for assistance with emission quantum yield measurements and thermal melting studies, respectively. We also thank Professor Christoph J. Fahrni (Georgia Institute of Technology) and Professor Jerry C. Smith (Georgia State University) for helpful discussions. Support of this research by the CICYT (Project BQU 2002-02576; A.L.), the National Science Foundation (Grant CHE-9984772; K.B.G.), the American Chemical Society Petroleum Research Fund (Grant 32897-G3; K.B.G.), and the Consejería de Educación de la Comunidad de Madrid (L.G.) is gratefully acknowledged.

Note Added after ASAP Publication. The heading of column 9 in Table 4 was corrected and other minor changes in the text were made to the version posted ASAP August 11, 2005; the corrected version was posted August 12, 2005.

Supporting Information Available: Chemical structures of the 3,6-acridinediamines **7**, **10**, acridine orange, and proflavin (Figure S1). This material is available free of charge via the Internet at http://pubs.acs.org.

IC048320X